REGULATION OF POLYHYDROXYALKANOIC ACID SYNTHASE BY RIBOSWITCH IN *CUPRIAVIDUS NECATOR*

KEITH LOGAN AUBREY
Bachelors of Arts and Science, Quest University, Canada 2018

A thesis submitted
in partial fulfilment of the requirements for the degree of

MASTER OF SCIENCE

in

BIOCHEMISTRY

Department of Chemistry and Biochemistry
University of Lethbridge
LETHBRIDGE, ALBERTA, CANADA

REGULATION OF POLYHYDROXYALKANOIC ACID SYNTHASE BY RIBOSWITCH IN CUPRIAVIDUS NECATOR

KEITH LOGAN AUBREY

Date of Defense: December 20, 2021

Dr. N. Thakor Thesis Supervisor	Associate Professor	Ph.D.
Dr. A. Zovoilis Thesis Examination Committee Member	Associate Professor	Ph.D.
Mr. T. Montina Thesis Examination Committee Member	Instructor	M.Sc
Dr. J. Hamel Chair, Thesis Examination Committee	Assistant Professor	Ph.D.

DEDICATION

To Linda Mofford, the best mother a son could hope for, whose constant support throughout my life has pushed me farther than I could have ever hoped, or deserved, to go. Most people don't get to meet their role models. I was born by mine

To Ramona Stinson, who never fails to tell me how proud she is of me and who consistently picks me up when I fall down. Her constant comfort and support helped me more than I think she realizes

Without these two beautiful people in my life, I doubt I would go as far as I have, and know I would not be as happy as I am. They both make me want to be a better person, and both make me believe I can be

ABSTRACT

Riboswitches provide an opportunity for inducible gene expression at the transcriptional and translational levels. The riboswitches utilized in this thesis function by creating secondary mRNA structures that sequesters the ribosome binding site (RBS), preventing translation. This secondary structure can bind to theophylline, causing the mRNA to refold, exposing the RBS and allowing translation to occur. Riboswitches are currently underutilized, tested in only a few model organisms and primarily explored through reporter genes for proof-of-concept. This thesis demonstrates the functionality of theophylline riboswitches in the industrially relevant bacteria *Cupriavidus necator*, and for inducible control of the industrially relevant enzyme polyhydroxyalkanoic acid synthase (phaC), both of which have previously not been demonstrated. This thesis tests the applicability of the riboswitch in industry-relevant bacteria and addresses a significant gap in the knowledge about riboswitch functionality.

ACKNOWLEDGEMENTS

A large thank you to Dr. Nehal Thakor, whose guidance and laboratory space made me enthusiastic to complete this work. I am incredibly thankful for his continued support and incredible knowledge throughout the years.

I am also incredibly grateful to my committee members Dr. Nehal Thakor, Dr. Athanasios Zovoilis, and Mr. Tony Montina, whose guidance and suggestions were invaluable throughout this process.

My laboratory companions, Dr. Joe Ross, Keiran Vanden Dungen, and Rachana Muley were also instrumental in a fun and productive laboratory environment. A special thank you to Dr. Ross for guidance and troubleshooting.

A huge thank you to RNA Innovation for the providing funding and opportunity through the Natural Sciences and Engineering Research Council (NSERC) Collaborative Research and Training Experience program (CREATE) Fellowship, as well as to the School of Graduate Studies (SGS) for their consistent support.

And a final thank you to the University of Lethbridge. Their classes, support, and guidance helped me throughout this journey.

TABLE OF CONTENTS

DEDICATION..... iii

ABSTRACT..... iv

ACKNOWLEDGEMENTS..... v

LIST OF TABLES..... viii

LIST OF ABBREVIATIONS..... x

1 Introduction..... 1

1.1 Overview of synthetic biology..... 1

1.1.1 Biological Devices..... 4

1.2 Overview of Riboswitches..... 5

1.2.1 Structure-Function of Riboswitches..... 6

1.2.2 Synthetic Riboswitches..... 7

1.2.3 The Theophylline Synthetic Riboswitch..... 8

1.3 Metabolic Engineering Through Synthetic Biology..... 9

1.3.1 Metabolic Engineering of *Cupriavidus necator* (H16)..... 10

2 Hypothesis and Objectives..... 14

3 Materials and Methods..... 15

3.1 Cloning..... 15

3.1.1 *C. necator* Plasmid Isolation..... 17

3.2 Fluorescence-activated Cell Sorting..... 18

3.3 PhaC Expression..... 19

3.3.1 Growth and Induction of phaC..... 19

3.3.2 Western Blotting..... 21

3.3.3 Gas Chromatography..... 22

4 Results and Discussion..... 24

4.1 Cloning Results…..... 24

4.1.1 Cloning Plasmid Constructs..... 24

4.1.1.1 pBADT-RboS-YFP Cloning..... 24

4.1.1.2 pBADT-RboS-phaC Cloning..... 26

4.1.2 Cloning Setbacks..... 28

4.1.2.1 Cryptic Bands Setback..... 28
4.1.2.2 *C. necator* Plasmid Isolation Setback..... 31
4.2 Riboswitch Functionality using Fluorescence Reporter Genes..... 32
4.2.1 Qualitative Imaging..... 33
4.2.2 Quantifiable Fluorescent Results..... 36
4.3 Riboswitch Functionality for Industrial Application..... 38
4.3.1 Analysis of PHB Standard..... 38
4.3.2 Growth Condition Optimization..... 40
4.3.3 Industrial Application of Riboswitch Variants..... 47
5 Study Strengths and Limitations..... 51
6 Conclusion..... 54
7 Future Directions..... 55
8 References..... 57
Appendix 1: Plasmid maps of pBADT-RboS-YFP & pBADT-RboS-phaC..... 65

LIST OF TABLES

Table 1: Sequences for synthetic theophylline riboswitch variants..... 15
Table 2: FACS data on fluorescent activity after gating..... 36
Table 3: Gas chromatography results for the standard experiment..... 39
Table 4: Gas chromatography results for preliminary experiment..... 41
Table 5: Gas chromatography results for optimization of L-arabinose and theophylline concentrations..... 43
Table 6: Gas chromatography results for PHB production through riboswitches.... 50

LIST OF FIGURES

Figure 1: Comparison of computer networks and living systems in synthetic biology..... 2
Figure 2: Schematic of a theophylline riboswitch structure-function relationship.... 9
Figure 3: Metabolic pathway for producing PHB in *C. necator*..... 11
Figure 4: The esterification of PHB into M3HB..... 13
Figure 5: Cloning process of pBADT-RboS-YFP plasmids..... 16
Figure 6: Cloning process of pBADT-RboS-phaC plasmids..... 17
Figure 7: Filter configuration used for the detection of YFP in FACS..... 19
Figure 8: Growth conditions for *C. necator* for phaC expression and PHB production..... 20
Figure 9: Extraction and preparation of PHB standard and samples..... 23
Figure 10: Conformational digest of pBADT-RboS-YFP plasmids from NEB5α.... 25
Figure 11: Attempted conformational digest of pBADT-RboS-YFP plasmids from *C. necator*..... 26
Figure 12: Conformational digest of pBADT-RboS-phaC plasmids from NEB5α... 27
Figure 13: Conformational digest of pBADT-RboS-phaC plasmids from *C. necator*..... 27
Figure 14: Investigating cryptic bands susceptibility to T5 Exonuclease..... 29
Figure 15: Investigating appearance of cryptic bands from glycerol stocks..... 29
Figure 16: Investigating cryptic band sizes between different isolated plasmids as well as the spontaneous appearance of bands from plasmid stocks..... 30
Figure 17: Investigating cryptic bands under numerous different conditions..... 30
Figure 18: Difficulties involving the isolation of plasmids in *C. necator*..... 32
Figure 19: Visual confirmation of inducible activity of the pBADT L-arabinose inducible promoter in *C. necator*..... 33
Figure 20: Investigation of riboswitch activity in *C. necator* through imaging..... 35
Figure 21: Quantification of riboswitch activity in *C. necator* through FACS..... 37
Figure 22: Chromatograph and analysis of PHB standards..... 40
Figure 23: Preliminary investigation of phaC expression and PHB production in *C. necator* controlled through a riboswitch..... 41
Figure 24: Optimization of induction, investigating L-arabinose and D-arabinose... 42
Figure 25: Optimization of induction concentrations for L-arabinose and theophylline (PHB Production)..... 44
Figure 26: Optimization of induction concentrations for L-arabinose and theophylline (phaC Expression)..... 46
Figure 27: Expression of phaC controlled by all riboswitch variants in *C. necator*.. 48
Figure 28: Production of PHB controlled by all riboswitch variants in *C. necator*... 50

LIST OF ABBREVIATIONS

CoA	coenzyme A
DCM	Dry cell mass
FACS	Fluorescence-activated cell sorting
GOI	Gene(s) of interest
GC	Gas chromatography
M3HB	3-hydroxybutyric acid methylester
mRNA	Messenger RNA
phaA	acetyl-CoA acetyltransferase
phaB	acetoacetyl-CoA reductase
phaC	polyhydroxyalkanoic acid synthase
PHB	Poly-3-hydroxybutyric acid
RboC	Synthetic theophylline riboswitch variant C
RboD	Synthetic theophylline riboswitch variant D
RboE	Synthetic theophylline riboswitch variant E
RboS	All synthetic theophylline riboswitch variants
RBS	Ribosome binding sequence
RFP	Red fluorescent protein
UTR	Untranslated region
WT	Wild type
YFP	Yellow fluorescent protein

1 Introduction

Synthetic biology provides a unique opportunity to modify organisms to help us deal with novel challenges. This section explains the concepts of synthetic biology, the development and use of biological tools in synthetic biology, expands on a specific biological tool; the riboswitch, and finally focuses on how the riboswitch could be used in the metabolic engineering of the industrially relevant bacteria *Cupriavidus necator* (H16).

1.1 Overview of synthetic biology

Although it was first coined back in the early 1900s, synthetic biology didn't significantly establish itself until recently and is therefore still an emerging discipline.[1,2] The field distinguishes itself as interdisciplinary, due to taking inspiration from other biological and non-biological disciplines.[1–4] Although synthetic biology uses a multitude of disciplines, it primarily expands upon the concepts of genetic engineering and combines those concepts with systems biology.[1,2] .

The approach of classical genetic engineering tends to focus on specific genes or gene clusters with an outcome directly related to the modification(s).[2] Systems biology, on the other hand, takes a bigger picture approach where the focus is on the entire living system, with the overall goal being a more profound understanding of living systems.[1,2] Synthetic biology combines these concepts, manipulating specific pathways and genes while observing the impact on the entire living system. To account for both the micro and macro aspects of living systems, synthetic biology has adopted a way for observing the organization of living systems that is inspired by computer sciences.[2,5,6]

Synthetic biology considers cells as programmable "physical" computers that can be programmed on the micro levels (such as its individual genes, gene products, and proteins) to impact the macro level (such as its overall metabolism, different pathways, phenotypes and even its environment) of a living system.[2,6] To simplify the organization of living systems, synthetic biology has taken to looking at organisms in a similar manner to how a computer scientist would look at computer networks.[2] In computer sciences a network consists of a hierarchy, broken down into a digestible manner; where the network is made up of computers; computers consist of modules inside the computer; modules use logic gates to dictate what the module does; and logic gates are made up of the physical components that allow electricity to pass through them. Inspired by this breakdown, synthetic biology also breaks down living systems into a similar hierarchy; where a living system is made up of tissues and/or cells; the function of the tissues and/or cells are completed by the pathways in the cells; the pathways are dictated by the different biochemical reactions; and the biochemical reactions consist of the physical components (proteins, genes, RNA, etc) that drive them (*Figure 1*). It is important to note that this analogy is not intended to be perfect. It does not account for feedback

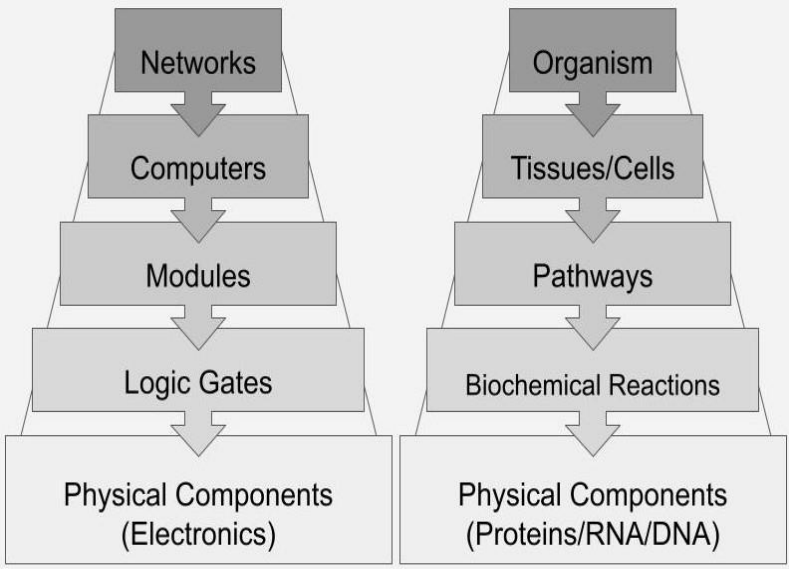

Figure 1: A side-by-side comparison of the breakdown of computer networks and living systems. The left-hand side deals with the breakdown of computer networks into their components and the right-hand side deals with the breakdown of living systems into its components.

loops, superorganisms, a living systems environment, or a variety of other things that help describe a living system. The analogy is used instead to help conceptualize the breakdown of an organism in this way that reduces complexity and allows a synthetic biologist to focus on both the narrow details (classical genetic engineering) as well as the big picture (systems biology).[2]

At its core, the goal of synthetic biology is to create what is sometimes referred to as the "industrialization" of biology.[1,7,8] The concept for the industrialization of biology is quite simple, it is to create biological systems that are significantly useful on an industrial scale,[1] however practical application of this is significantly challenging. An effective approach that synthetic biology has taken to is the modification or extension of an organism's behaviour.[2] Thinking about the hierarchy described above, behavioral changes would be found at the upper levels of the hierarchy, at or even above the organism level, but would need to be implemented bottom-up, at the lower levels of the hierarchy.[2] As synthetic biology considers living systems as programmable physical computers,[2,6] it attempts to program these lower levels using different tools and techniques.

To program these changes, synthetic biology tackles the issue on multiple fronts using different disciplines in a "design-build-test-learn" cycle.[4] To tackle a problem, first comes design, where disciplines such as systems biology can help guide decision making for a potential solution. [1,2,4] Lastly, disciplines such as mathematics and bioinformatics can develop informative algorithms and analyze data, which can then be used to inform better design solutions and the cycle can begin again, building on each iteration..[1,2,4] The disciplines stated here are not exhaustive or restricted to a certain part of a design-build-

test-learn cycle, however this serves as an example of how multiple disciplines can work together for a solution.[1,2,4]

1.1.1 Biological Devices

A key aspect of synthetic biology is to make biology easier to engineer by creating complex systems while simultaneously reducing complexity into a digestible manner.[2,4,5,9] One way this is accomplished is through the use of biological devices (also referred to as biological tools).[2,10,11] The definition of a biological device is abstract, but fundamentally they are basic design "units" that can be put together in a system for complex results.[2,10,11] Biological devices can control biological functions by responding to inputs and generating outputs in the system, and can do so in a wide range of processes such as (but not limited to) translation, transcription, phosphorylation, ligand/receptor binding, and enzymatic reactions.[2]

An important feature of a biological device is the ability to assemble them into what are often referred to as circuits. Biological circuits use a series of simple biological devices to help modify an organism.[2,10,11] Through this, complex modifications can be made using simple, often single use, devices. The biobrick is a good example of a biological device. Biobricks are easily clonable genetic sequences that perform functions such as phosphorylation, inducible transcription, production of enzymes or more. By using biobricks, complex modifications can be designed and made through basic molecular cloning practices.[12]

Research and development for biological devices is slow and difficult, requiring significant experimental biology and computational design to understand the contexts and details on how these devices function.[2,13] Because each living system is different, certain

tools that may be useful in one system may be non-functional in another. Discovering and characterizing reliable and universal tools is required to fully take advantage of this field.[13] Regulating inducible expression is a common goal in synthetic biology, however finding biological devices capable of doing this is difficult.[14] Although there has been success with the development of synthetic gene clusters,[14] far more powerful biological devices are simpler and more reliable, with modular capabilities that can be moved into new organisms without requiring as many supporting factors.[2,10] This thesis will focus on characterizing and demonstrating the use of the riboswitch, an RNA regulatory element that can be used as a biological device.[15]

1.2 Overview of Riboswitches

The riboswitch is a three-dimensional structure formed in RNA, which was first experimentally confirmed in bacteria in 2002.[16–18] Riboswitches are RNA elements capable of impacting gene expression through the modulation of an expression platform, commonly induced by the binding of a ligand to what is referred to as the aptamer domain. The exact mechanism for this is explained in the "1.2.1 Structure-Function of Riboswitches" section. Riboswitches are organized into two categories, family and class.[19] Both family and class refer to aspects of the aptamer domain. The family of the riboswitch refers to which ligand it binds to, while the class of the riboswitch refers to the shape of the aptamers, and can usually be identified by common sequence patterns.[19] As of 2017, nearly 40 different classes of riboswitches have been reported on, it is predicted and very likely that thousands of riboswitches have yet to be discovered.[20]

1.2.1 Structure-Function of Riboswitches

Riboswitches operate through conformational changes in RNA sequences caused by a multitude of different variables. These variables are typically metabolites, but riboswitches can also respond to complementary nucleic acids that use conventional Watson-Crick base pairing (referred to as a toehold switch) as well as thermosensing switches that respond to temperature.[21,22] Riboswitches are *cis*-acting elements generally located at the 5' UTR, however, the discovery of the 3' UTR located thiamin pyrophosphate riboswitch indicates that there may be more undiscovered 3' located switches.[21,23] Riboswitches can also form a multitude of tertiary structures, the two most common being pseudoknot-like structures and three-way junction structures.[21] Despite riboswitch variety in their inducible triggers, locations, and structures, all known riboswitches can be broken down into two main regions; the aptamer domain and the expression platform. These two regions work together to dictate gene expression in response to environmental or cellular signals.

The area that instigates conformational change in the RNA's structure is referred to as the aptamer domain, which is a fairly conserved evolutionary feature.[20,24] This domain functions by containing a structure capable of responding to an external or internal signal, commonly by containing a binding pocket for a ligand. In the ligand-bound state (or equivalent), the RNA adopts a conformational change which impacts the second domain; the expression platform. Compared to the aptamer domain, the expression platform of a riboswitch is not as evolutionarily conserved and is known to have much more variability.[20,24] The expression platform responds to the conformational change triggered by the aptamer domain, and induces or represses expression typically by regulating

transcription, translation, or less often through alternative splicing.[21,23,25] Although many of these riboswitches have been found in nature, we have also created a range of synthetic riboswitches that use different mechanisms and are capable of responding to a variety of ligands.[26]

1.2.2 Synthetic Riboswitches

Traditionally, the production of useful compounds from organisms utilizes inducible promoters to control gene expression on the transcriptional level, and as previously discussed this can require entire gene clusters to function properly. Synthetic riboswitches provide an attractive alternative to this as their inducible system tends to rely solely on the interaction between the aptamer domain and its ligand (or equivalent), without requiring supporting cellular machinery to function. One of the most promising aspects of synthetic riboswitches is how effectively they can be designed or improved. There has been significant success designing synthetic riboswitches through both screening randomized or semi-randomized sequences and using computer modelling and rational design.[15] There has been success through the use of trial and error screening and semi-randomized methods in designing and/or improving upon riboswitches, such as improving upon the theophylline riboswitch.[27,28]

Synthetic riboswitches have been used mostly for proof-of-concept experiments in *E. coli* using reporter genes,[21] but they have been used for limited practical applications as well. Riboswitches have been deployed in biofuel production, gene therapy, bioremediation and more.[15,21,29] To our knowledge, riboswitches have neither been introduced into *C. necator* nor have they been used for industrial plastic applications. This is the cornerstone of this thesis work, to better characterize riboswitches by placing them in a novel,

industrially relevant, context. In particular, theophylline-dependent riboswitches will be investigated in an unexplored model organism controlling genes involved with plastic production.

1.2.3 The Theophylline Synthetic Riboswitch

Multiple variants of synthetic theophylline-dependent riboswitches were developed and provided to us by the laboratory of Dr. James Golden (Department of Biological Sciences, University of California San Diego).[30,31] Each of the synthetic riboswitch variants were based on two synthetic theophylline riboswitches that had been previously discovered.[32] The riboswitches were discovered by screening a library using a variety of different screening techniques, including blue-white selection, mobility assays, and flow cytometry. These two riboswitches were discovered based on their low levels of leaky expression (expression without induction) and high theophylline sensitivity. Once discovered the riboswitches were 5'-end radiolabeled for imaging using T4 polynucleotide kinase and [γ-^{32}P]ATP, structurally probed using T1 nuclease, and analyzed using the RNA secondary structural predicting software *mFold* to determine their structure-function.[32] The riboswitches operate by forming a secondary structure in the mRNA which sequesters the ribosome binding site (RBS), thus preventing gene expression on the translational level. This secondary structure contains a ligand-binding aptamer domain that binds to theophylline, causing the mRNA to refold in such a way that the RBS is exposed, allowing translation to proceed (*Figure 2*).[15,30] This provides the riboswitches with significant plug-and-play versatility, as its inducible function is based on the interaction of the ligand to the riboswitch aptamer.[15,32]

Based on the sequence and structure the two above-mentioned synthetic riboswitches,[32] other variants were designed using a combination of *in vivo* screening and rational design.[30] These different variants were tested in a multitude of different organisms with varying degrees of successful expression and low levels of leaky expression.[30,31] Three of these variants (variant C, variant D, and variant E) are the basis of this thesis work.

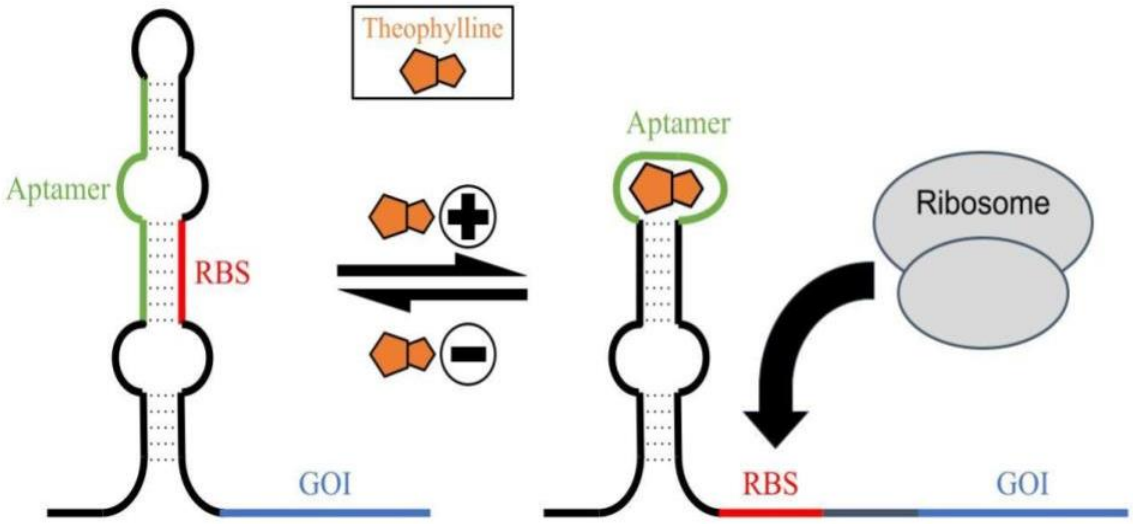

Figure 2: A simplified schematic diagram of a theophylline riboswitch structure-function relationship. When in the unbound state, the riboswitch forms a hairpin structure sequestering the RBS and preventing translation from occurring. When in the theophylline bound state, the structure refolds, exposing the RBS and allowing translation to occur.

1.3 Metabolic Engineering Through Synthetic Biology

Metabolism refers to all the biochemical processes performed by an organism, and utilizes two primary mechanisms; catabolic pathways (degradative pathways that break organic nutrient molecules such as carbohydrates and lipids) and anabolic pathways (pathways that biosynthesize precursors into larger, more complex molecules for the organism).[33] Often these processes can produce metabolites that prove to be useful resources, and using living systems for production of these resources has been occurring for centuries, however, the engineering of organisms for this purpose is relatively recent.[34] Metabolic engineering initially focused on specific pathways that

would produce desired metabolites, the approach of observing the metabolic flux within the entire organism has more recently been embraced, an approach coined systems metabolic engineering.[34]

Systems metabolic engineering uses tools and strategies from systems biology, evolutionary engineering, and synthetic biology to produce both natural and non-natural resources.[35–37] The combination of strategies and tools from these fields, such as (but not limited to) pathway prediction algorithms from systems biology, directed evolution from evolutionary engineering, and gene expression tools from synthetic biology) can be used in tandem to to create highly preformative microbial factories.[35,37] These cellular "factories" have produced medicinal products such as poly(lactate-co-glycolate) and opioids,[37–39] as well as chemicals such as isopropanol and butanol.[36,40,41]

Although the shift to systems metabolic engineering greatly increased the finesse in which we could engineer metabolism, systems metabolic engineering can still be improved upon as there is a lack of universally applicable tools for metabolic manipulation in different living systems, a problem that synthetic biology specifically focuses upon.[34]

1.3.1 Metabolic Engineering of Cupriavidus necator (H16)

This thesis focuses on the ability of synthetic theophylline riboswitches to control gene expression in *Cupriavidus necator*. This bacteria is of industrial interest due to numerous factors, such as heavy metal resistance[42,43] and its ability to break down waste products.[44] One of the greatest characteristics of this bacteria is its capability to produce and accumulate bioplastics at industrially relevant concentrations.[45] Bioplastics are biodegradable polymers produced from renewable sources,[46] with numerous different species capable of producing them.[47] *C. necator* is an organism of note in this regard due to its capabilities to produce the bioplastic Poly-3-hydroxybutyric acid (PHB) at concentrations of up to 70% to 80% of its dry cell mass (DCM).[45,48,49]

C. necator uses glucose as an energy and carbon resource, producing pyruvate through glycolysis, from there it produces PHB through a series of enzymatic reactions (*Figure 3*). Pyruvate and coenzyme A (CoA) combine with the help of NAD^+ to produce acetyl-CoA and NADH. From there, acetyl-CoA acetyltransferase (phaA) converts Acetyl-CoA into Acetoacetyl-CoA, which is converted into *R*-hydroxybutyryl-CoA by acetoacetyl-CoA reductase (phaB), and lastly, PHB is produced from *R*-hydroxybutyryl-CoA via polyhydroxyalkanoic acid synthase (phaC).[51]

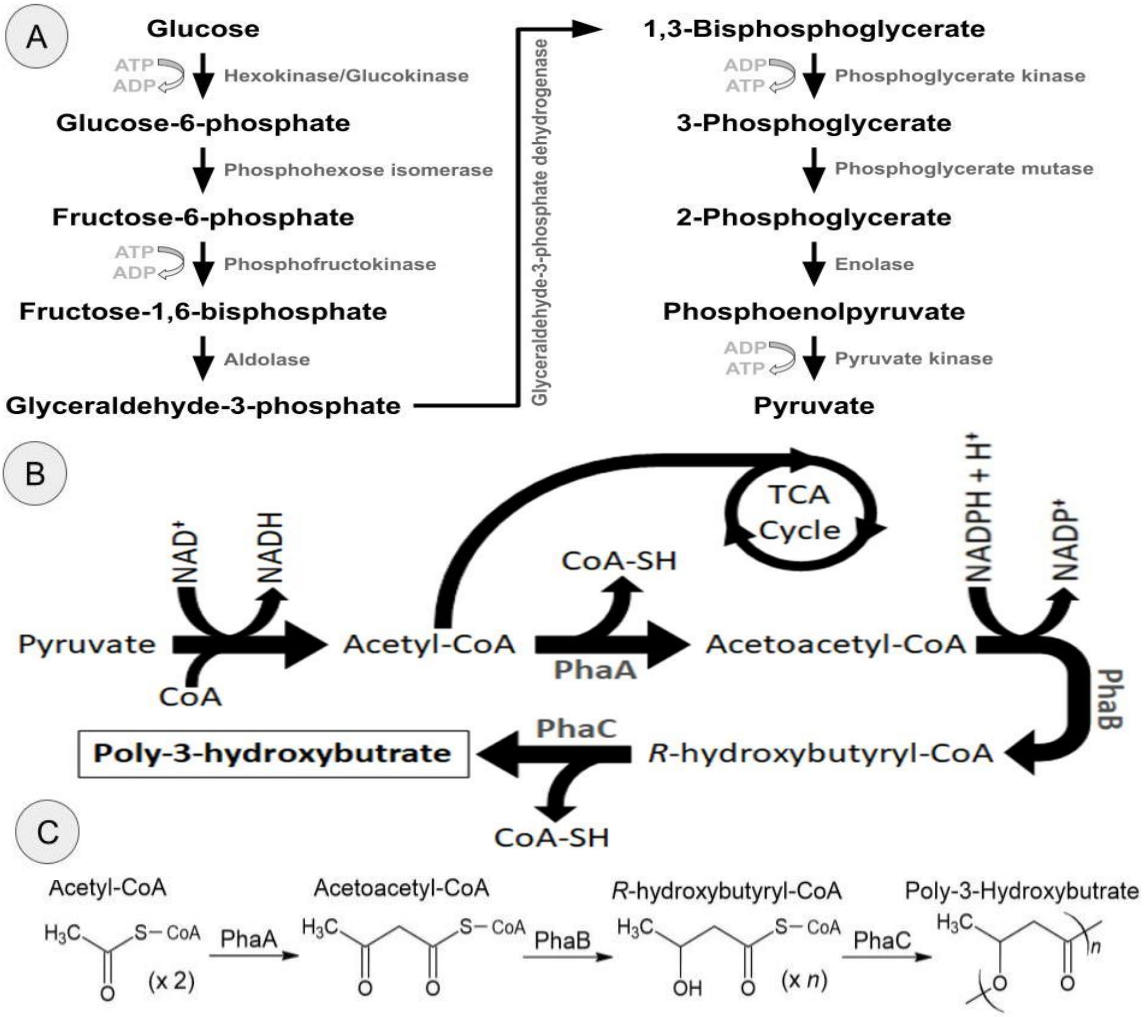

Figure 3: Relevant pathways and molecular structures in the *C. necator* PHB pathway. A) The glycolysis pathway from glucose to pyruvate.[50] B) The metabolic pathway for producing PHB in *C. necator*, starting from pyruvate.[51] C) Relevant molecular structures in the PHB pathway.[51]

This metabolic pathway can be heavily encouraged through nutrient limitation, which causes *C. necator* to redirect carbon metabolism from growth and replication pathways into this resource storage pathway.[51–53] Under nutrient limited growth conditions *C. necator* accumulates PHB for both carbon and energy storage.[52] This is due to nutrient limitation causing an increase in NADH/NAD ratios in the cell. Acetyl-CoA can either enter the tricarboxylic acid (TCA) cycle or act as a precursor for acetoacetyl-CoA in PHB synthesis. An increase in the NADH/NAD ratio inhibits citrate synthase, which in turn inhibits acetyl-CoA from entering the TCA cycle, causing it to be used for PHB production instead.[54] Nitrogen limitation, in combination with excess carbon, is a common growth condition for the accumulation of PHB.[53,55–58]

After *C. necator* produces PHB, it can be isolated through solvent extraction, such as chloroform extraction and solvent-hypochlorite dispersion extraction.[59] For chloroform extraction, the cells are stirred in chloroform followed by an ethanol precipitation.[59] Solvent-hypochlorite dispersion extraction can use a variety of organic solvents, in which the wet biomass is first treated with a dispersion solution, pelleted, and then incubated with the organic solvents before being centrifuged and recovered from the organic phase. Although this method is more complex and time consuming, it generates better yield than the chloroform extraction method. The organic solvent used is also impactful, as ethylene carbonate demonstrated higher yield than six other organic solvents.[59] After extraction, PHB can be used for the manufacturing of thermoplastics. *C. necator* can produce PHB with a range of degree in crystallinity (over 20% to over 60%),[60,61] as well as a molecular mass of over 300,000 Da.[61] However, both crystallinity and molecular mass can be changed through enzymatic treatment to create plastics catered to different industrial needs.[61]

For research purposes, the objective is often to quantify the amount of PHB in a *C. necator* culture rather than converting it into usable bioplastics for industrial manufacturing. For this, common method is to break PHB into a esterified monomer form, 3-hydroxybutyric acid methylester (M3HB), using a methanol/chloroform/sulfuric acid solution. This solution is added to the cells at a high temperature, destroying the cells and cells and allowing the solution to esterify the PHB.[62–64] M3HB is created through acidic methanolysis, which is a stepwise reaction in which PHB interacts with methanol catalyzed by sulfuric acid (*Figure 4*).[62–64] This reaction serves two primary purposes, to isolate PHB and to convert it into a form easily analyzed through gas chromatography. PHB chains can exist in a wide range of lengths,[65] which would cause numerous peaks in gas chromatography if untreated. Breaking these chains into M3HB monomers condenses the signal into one peak. M3HB is also volatile in gas chromatography conditions, and interacts with the solid phase of GC easily, making it attractive for GC analysis.[62]

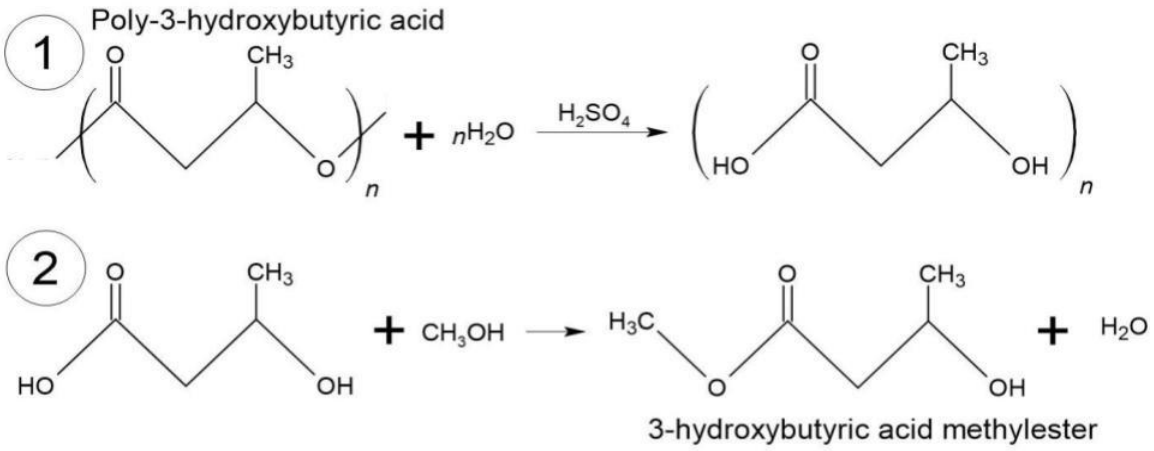

Figure 4: The esterification of PHB into M3HB monomers. Catalyzed through sulfuric acid, PHB is first broken into smaller chains which can then interact with methanol to create M3HB.[41]

2 Hypothesis and Objectives

This thesis attempts to demonstrate the use of synthetic theophylline-dependent riboswitches in industrial application. For this, three synthetic theophylline riboswitches variants were cloned into plasmids upstream of (and in control of) a phaC gene, before being transformed into a ΔphaC *C. necator* strain. This places these synthetic theophylline riboswitch variants in two novel contexts yet to be characterized. The first novel context is in the model organism *C. necator*, which to our knowledge has yet to demonstrate compatibility with riboswitches. The second novel context is the control of the expression of phaC for PHB production, which to our knowledge has also not been demonstrated before. This serves to test the modularity of the riboswitch as well as pushing the limitations of current literature. As the synthetic riboswitches used in this thesis have been shown to function in a diverse range of bacteria,[30,31] and due to the plug-and-play nature of riboswitches,[14,15,21] we hypothesize that these synthetic riboswitches are capable of gene expression in *C. necator* and can be used to produce industrially and environmentally relevant products. To demonstrate this my objectives are as follows:

OBJECTIVES

***Overarching goal*:** To demonstrate the potential of riboswitches as useful biological devices in industrial applications.

***Specific aims*:** (1) Regulation of gene expression in *C. necator* using theophylline riboswitches. (2) Expression of the industrially relevant enzyme phaC controlled by theophylline riboswitches in a ΔphaC *C. necator* strain. (3) Production of PHB in ΔphaC *C. necator* controlled by theophylline riboswitches.

3 Materials and Methods

3.1 Cloning

Two sets of plasmids containing either the florescent reporter gene YFP or phaC as the gene of interest (GOI) were cloned downstream of all theophylline riboswitch variants (RboS), which consisted of variant C (RboC), variant D (RboD), and variant E (RboE) (*Table 1*). Both YFP and phaC contained a cmyc tag fused to their N-terminus, which is a small protein tag commonly used for western blotting. The cmyc tag was intentionally included for western blotting purposes as well as because initial plasmid constructs were provided to us by Dr. Golden which also included the tag. Inserts were cloned into a pBADT vector at the XbaI and BamHI sites using a pBADTrfp (Addgene; 99382) plasmid, in which red fluorescent protein (RFP) was removed during this process (*Figure 5* & *Figure 6*). NEB5α (CAT# C2987H) was used as a maintenance strain during the cloning process before being transformed into *C. necator* or ΔphaC *C. necator*. Both *C. necator* strains were gifted to us by Drs. Steffen Schaffer and Markus Pötter (Evonik Creavis GmbH).

Table 1: The sequences for the synthetic riboswitch variants including the cmyc tag. Sequences highlighted in green indicate the riboswitch sequence, sequences highlighted in yellow indicate the cmyc tag, and the location of the GOI (either YFP or phaC) is highlighted in red. Start codon is bolded and underlined.

RboS	**Sequence (5' → 3')**
RboC	TGATAAGATAGGGGTGATACCAGCATCGTCTTGATGCCCTTGGCAGCACCAAGGGACAACAAG**ATG**GAACAAAAACTGATTAGCGAAGAAGATCTGACAAGTTTGTACAAAAAAGCAGGCTCCGCGGCCGCCCCCTTCACC-GOI
RboD	GGTGATACCAGCATCGTCTTGATGCCCTTGGCAGCACCCTGCTAAGGTAACAACAAG**ATG**GAACAAAAACTGATTAGCGAAGAAGATCTGACAAGTTTGTACAAAAAAGCAGGCTCCGCGGCCGCCCCCTTCACC-GOI
RboE	GGTGATACCAGCATCGTCTTGATGCCCTTGGCAGCACCCTGCTAAGGAGGTAACAACAAGATGAATTC**ATG**GAACAAAAACTGATTAGCGAAGAAGATCTGACAAGTTTGTACAAAAAAGCAGGCTCCGCGGCCGCCCCCTTCACC-GOI

For pBADT-RboS-YFP constructs, the laboratory of Dr. Golden provided us three plasmids; pAM5046, pAM5047, and pAM5048 (containing RboC-YFP, RboD-YFP, and RboE-YFP respectively[31]). These were used to create the inserts through PCR with primers containing tags with the appropriate restriction sites. PCR products were then digested and cleaned up through a Qiagen PCR Cleanup kit (CAT# 28106) before being ligated into the digested pBADT vector (*Figure 5*). Ligated material was then transformed via heat shock into NEB5α and confirmed through restriction digestion.

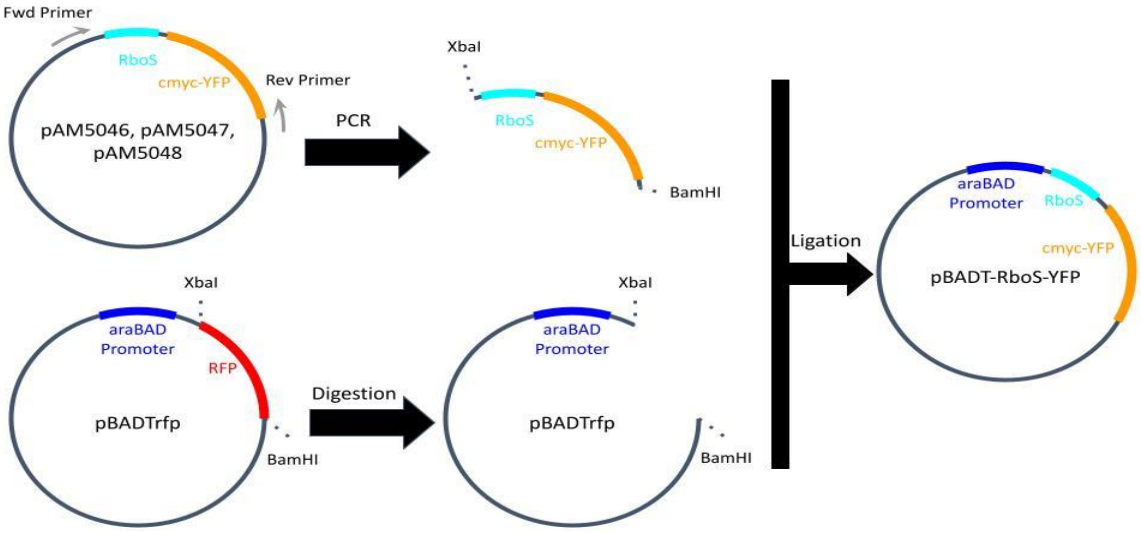

Figure 5: Schematic of the cloning process. Primer sequences highlighted in green indicate the annealing region and sequences highlighted in red represent restriction sites for XbaI (Forward primer) and BamHI (Reverse Primer). Each plasmid contains a different riboswitch variant (RboC, RboD, or RboE) but are otherwise identical. Constructs were designed with a cmyc tag fused to the N-terminus of YFP.

For pBADT-RboS-phaC constructs, RboC-phaC, RboD-phaC, and RboE-phaC were synthesized by Genewiz (115 Corporate Boulevard, South Plainfield, NJ 07080) into pUC-GW vectors, which already contained appropriate restriction sites. Synthesized Genewiz plasmids were digested and ligated into the digested pBADT vector (*Figure 6*) without cleanup. Ligated material was then transformed via heat shock into NEB5α and confirmed through restriction digestion.

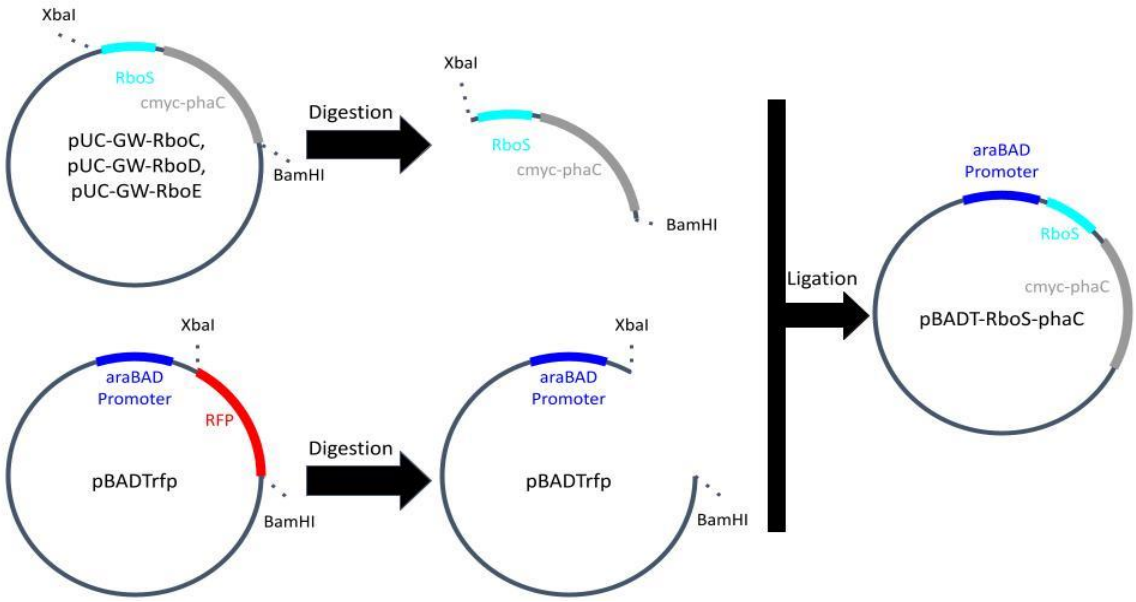

Figure 6: Schematic of the cloning process. Plasmids were digested and ligated together without clean-up and multiple colonies were picked until restriction digestion confirmed correct plasmid constructs. Each plasmid contains a different riboswitch variant (RboC, RboD, or RboE) but are otherwise identical. Constructs were designed with a cmyc tag fused to the N-terminus of phaC.

Plasmid maps for pBADT-RboS-YFP and pBADT-RboS-phaC can be found in *Appendix 1*. Once plasmid constructs were confirmed through restriction digestion in NEB5α, pBADT-RboS-YFP and pBADT-RboS-phaC constructs were transformed through electroporation into *C. necator* and ΔphaC *C. necator* respectively. Once transformed, another conformation through restriction digestion was attempted.

3.1.1 C. necator Plasmid Isolation

C. necator was cultured overnight in 4 - 5 mL LB culture tubes containing kanamycin. 1.5 mL of the overnight culture was then pelleted in a 1.5 mL centrifuge tube at 12,000xg for 2 minutes. The LB supernatant was decanted and the pellet was resuspended in a 100 µL Resuspension Buffer containing 25 mM Tris-HCl, 10 mM EDTA, and 100 µg/mL RNase A, with a pH of 8.0. Once resuspended, 100 µL of a Lysis Buffer

containing 200mM NaOH and 1% SDS was added and the tube was gently inverted 5-6 times before being incubated at room temperature for 3 minutes. After incubation 120 µL of a Neutralization Buffer containing 3M Potassium Acetate at 5.5 pH using Acetic Acid was added and the tube was gently inverted 5-6 times before being incubated at room temperature for 3 minutes. The tubes were then pelleted at 12,000xg for 2 minutes after which the supernatant was transferred to fresh 1.5mL centrifuge tubes. 200µL of 95%-99% isopropanol was added and thoroughly mixed via inversion 10-15 times before being incubated at room temperature for 2 minutes. After incubation, the DNA was pelleted at 16,000xg for 2 minutes and the supernatant was decanted. 500µL of 70% ethanol was added and mixed via gentle pipetting until the DNA pellets were dislodged. The DNA pellets were pelleted again at 16,000xg for 2 minutes, after which the supernatant was decanted and the tubes were then air-dried by placing them upside down with their caps open on a clean paper towel. Once dry, the DNA was resuspended in 20 µL of sterile water and stored at -20°C.

3.2 Fluorescence-activated Cell Sorting

Cultures were grown overnight in LB containing kanamycin and inducible conditions (0.001% (wt/vol) L-arabinose and/or 2 mM theophylline) at 30°C and 250 rpm. Cultures were then centrifuged at 12,000 xg for 1 minute and washed 3 times with 1x PBS containing 0.1% BSA before being resuspended in the PBS/BSA mixture and placed on ice. Cultures were transported on ice to the University of Calgary for fluorescence activated cell sorting (FACS) analysis using the Attune NxT instrument by Thermo-Fisher. YFP

fluorescence was read through the fluorescein isothiocyanate (FITC) channel which uses a 488 nm wavelength laser for excitation. YFP signal was detected through a 495DLP mirror and 503LP filter, reflected by a 555DLP mirror, and finally detected through a 530/30 bandpass filter (*Figure 7*). Results were analyzed through the Attune NxT Software V4.2.0. Manual gating was used for both all events and for fluorescence activity.

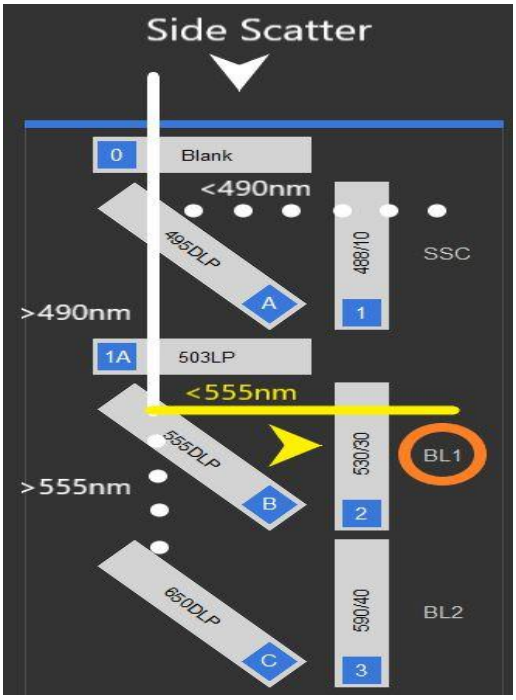

Figure 7: Filter configuration used for FACS for the detection of YFP using the BL1 detector in the Attune NXT instrument. The illustrated pathway is referred to as the FITC channel for the machine.

3.3 PhaC Expression

3.3.1 Growth and Induction of phaC

Primary cultures were grown in LB containing kanamycin overnight at 30°C and 250-300 rpm in baffled flasks. The primary culture was then used to inoculate (at 1/10th final volume) a secondary culture of M9 media containing L-arabinose and theophylline at concentrations that varied between experiments. These secondary cultures were grown at 30°C and 250 - 300 rpm in baffled flasks for 24 hours to deplete nitrogen within the M9 media. After 24 hours, 20% glucose was added (at 1/10th final volume) to the cultures to create nitrogen limited conditions to act as the nutrient deficient condition, alongside excess carbon to encourage PHB formation. Cultures were then incubated for another 24 - 48 hours before harvesting. For cultures that grew for an additional 48 hours, glucose was added again to ensure excess glucose through growth (*Figure 8*).

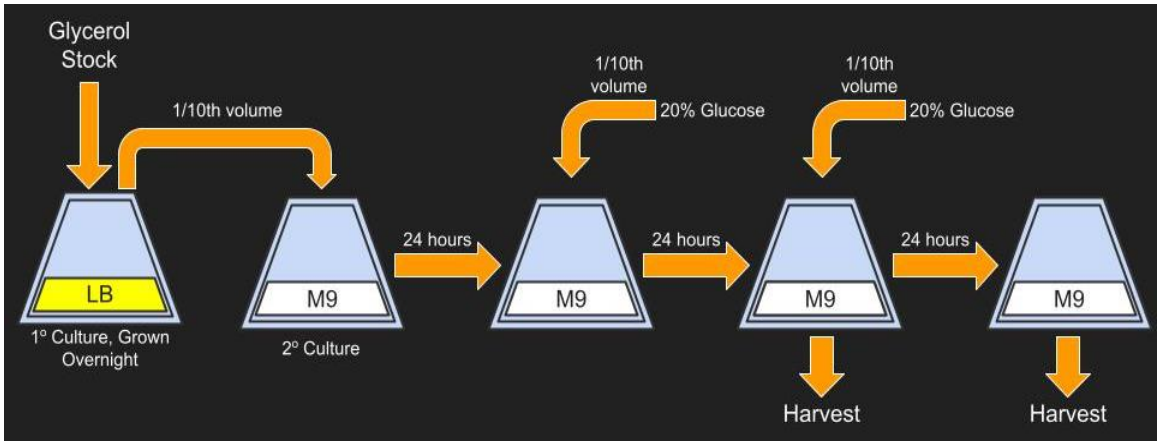

Figure 8: Growth conditions for *C. necator* for phaC expression and PHB production. If 2° culture was harvested after 48 hours (first harvesting point) no excess glucose was added.

For harvesting, 10 mL of culture was initially used and transferred to 15 mL conical centrifuge tubes. Later, for more dry cell mass, 45 mL of culture was used and transferred to 50 mL conical centrifuge tubes. From there, the cultures were centrifuged at 6000 xg for 10 minutes. Supernatant was decanted and pellets were then resuspended in 1 mL PBS and split into two separate centrifuge tubes of equal volume (500 µL each). One tube was used for western blotting (see 3.3.2 Western Blotting) while the other tube was used for gas chromatography (see 3.3.3 Gas Chromatography). After resuspension in PBS, cells were centrifuged at 12,000 xg for 2 minutes. Supernatant was decanted and pellets were washed in either PBS (for western blotting) or water (for GC) before being centrifuged again at 12,000 xg for 2 minutes. Supernatant was decanted and centrifuge tubes were placed upside down with their lids open until the pellets were relatively dry. Samples were then placed at -80°C for storage (16 - 72 hours) before being prepped for either western blotting or lyophilized for gas chromatography (GC).

3.3.2 Western Blotting

Western blot protocol was adapted from previously published methods.[66] The frozen pellet from "Growth and Induction of phaC" was thawed and resuspended in 500 µL of a lysis solution (50 mM Tris, 1 mM EDTA, 2% SDS, pH 8) before snap freezing at -80°C for 5 minutes. The lysate was then partially thawed, vortexed for 5 seconds, and placed on ice for 10 minutes Vortexing and ice treatment was repeated 3 times. The lysate was then centrifuged at 4°C for 10 minutes at 10,000 xg. The lysate (supernatant) was removed and stored at -20°C, the pellet was discharged. 2.5 µL of the lysate was mixed with 250 µL of Bradford reagent, vortexed 3 times for 5 seconds each, before 200 µL of the mixture was pipetted into a 96 well plate removed from light. Total protein content was determined by scanning the 96 well plate with a Cytation 5 plate reader. Using the results from the Bradford assay, protein lysate was then prepped for western blotting by mixing the lysates with water to create a sample containing equal amounts of protein (20 µg to 30 µg of total protein). The sample was then mixed with a 5 times concentrated protein loading dye (312.5 mM Tris HCl, 10% SDS, 25% Glycerol and 5% β-mercaptoethanol) and heated at 95°C for 20 minutes before being loaded onto 10% protein gels and ran at 120 Volts for 80 - 120 minutes. Samples were then transferred to a nitrocellulose blotting membrane using 110 Volts for 1 hour.

After transfer, blots were exposed to Ponceau Stain (5% acetic acid and 0.1% Ponceau Dye) briefly (1-3 minutes) and imaged using Amersham Imager 600. Total protein amounts from ponceau were used to normalize western blotting results. Ponceau was washed off before blocking with 10% milk (in 0.1% PBST) for 1 hour at 4°C on a rocker. Afterwards, the milk was decanted and the blots were washed with 1x PBS before being

exposed to the primary antibody (Myc-Tag Rabbit mAb from NEB (CAT# 2278S), diluted to distributor's recommendation in 1% Milk, 0.1% PBST, and 0.1% NaAzide) overnight at 4°C on a rocker. Primary antibody was decanted and blots were washed on a rocker 6 times with PBS containing 0.02 % (v/v) Tween 20 for 5 minutes. Blots were then exposed to secondary antibody (Goat Anti-Rabbit IgG from Abcam (CAT# ab97051), diluted to distributor's recommendations in 1% milk and PBS containing 0.1 % (v/v) Tween 20) for 1 hour at 4°C on a rocker. Secondary antibodies were then decanted and blots were again washed on a rocker 6 times with PBS containing 0.02 % (v/v) Tween 20 for 5 minutes. Blots were then treated with Pierce ECL Western Blotting Substrate from Thermo Scientific (CAT# 32106) following distributor's protocol, before being analyzed with an Amersham Imager 600.

3.3.3 Gas Chromatography

The frozen pellet from "Growth and Induction of phaC" was lyophilized overnight at a vacuum pressure of ~0.07 mbar and a temperature of -50°C, before being placed at -80°C for storage, with no further drying of the cells being conducted. Cells were thawed and an equal weight (1 - 3 mg) of dry cell mass was transferred into large glass screw-cap tubes (25 mL). For standard and/or reference samples, a 0.5 or 1 mg/mL solution of PHB powder from Sigma-Aldrich (CAT# 363502-10G) dissolved in chloroform was used in replacement of the dry cell mass. The PHB/chloroform solution was made by heating the solution to 55°C until the PHB was dissolved, mixing occasionally. 10 - 100 µL of the PHB/chloroform was used to create the standard and/or act as a reference sample, with the amount of PHB/chloroform used for each of the ladders specified in each experiment. 100 µL of pure chloroform was used for negative controls. The dry cell mass,

standard/reference, and negative control were then incubated in 3 - 5 mL of a chloroform/methanol/sulfuric acid solution (in a ratio of 1/1.7/0.3 respectively) for 1 hour at 100°C (briefly mixed every 20 minutes). Afterward, the mixture was cooled to room temperature, an equal volume of water was added, the mixture was vortexed briefly, and left at room temperature for phase separation. A glass disposable pipet was then used to transfer the bottom organic layer to a gas chromatography glass vial for GC analysis (*Figure 9*).

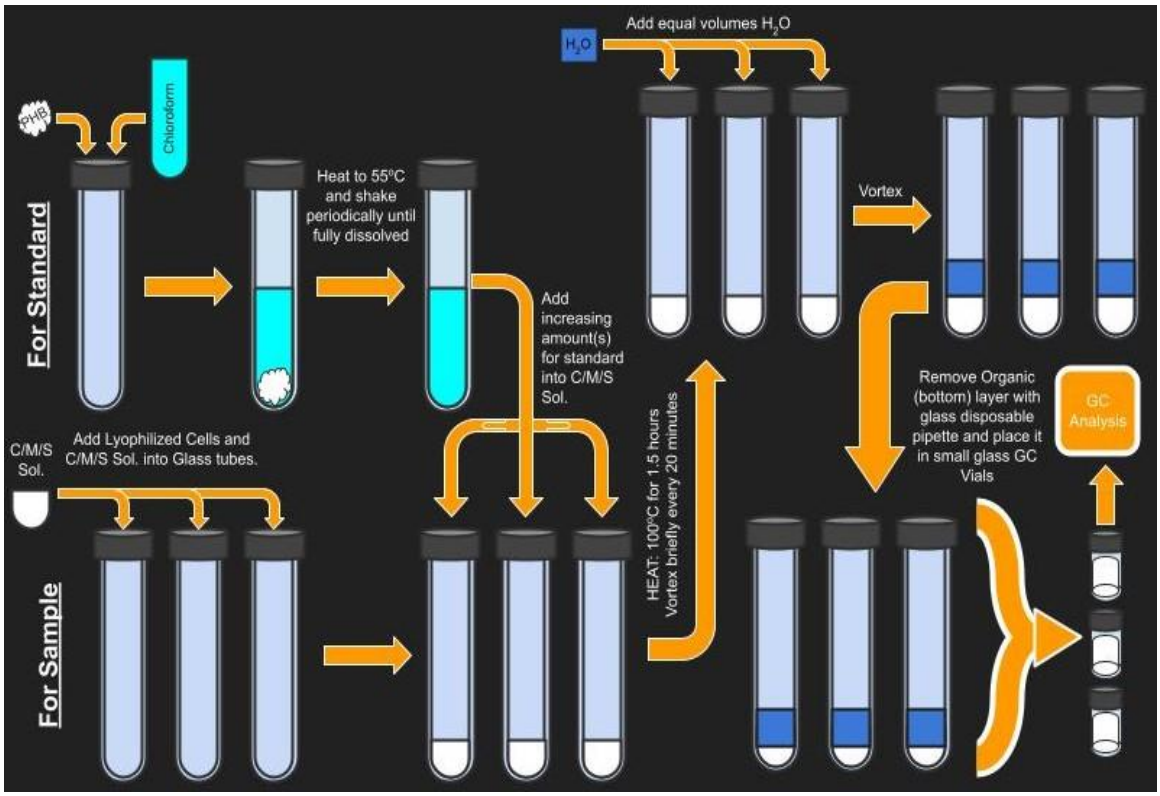

Figure 9: Extraction and preparation method of PHB standard and samples. C/M/S Sol. indicates the chloroform/methanol/sulfuric acid solution used for extraction.

GC analysis was conducted using a Varian Chrompack CP-3800 with a CP-8400 Autosampler (Injector 1177, 10 µL syringe). GC analysis was conducted on each sample three times. The injection volume set to 1 µL, the column was 15 M, with a 0.25 mM diameter and consisted of a VF-23ms stationary phase from Agilent at 0.25 µM thickness.

Column flow rate was set to 2 mL/min with 10 mL/min purged out of the split vent (for a split ratio of 5). The hydrogen carrier gas consisting of nitrogen, hydrogen, and dry air (ratio of 5/28/300 respectively). Oven temperature was set at 60°C for 2 minutes followed by an increase of 10°C per minute to 200°C (total time 16 minutes). Washes consisted of 5 µL methanol followed by 5 µL of iso-octane, performed once before sampling and twice after sampling. With these settings, the peak occurred at around the 2.7 minute mark (confirmed by the standard/reference). Results were analyzed using the Scion Instruments CompasCDS Ver. 4.1.0.296, and the area under the peak was used to determine the signal in µvolts per minute (µV.Min).

4 Results and Discussion

4.1 Cloning Results

4.1.1 Cloning Plasmid Constructs

Two sets of plasmids were cloned containing either YFP or phaC as described in Materials and Methods. These sets each consisted of three riboswitch variants placed upstream of the GOI, for a total of six plasmids. The first set contained RboC, RboD, and RboE upstream of YFP. This set was used to determine riboswitch activity using a reporter gene. The second set contained RboC, RboD, and RboE upstream phaC. This set was also used to determine riboswitch activity as well as to determine the industrial potential of the riboswitches.

4.1.1.1 pBADT-RboS-YFP Cloning

RboS-YFP inserts were cloned into a pBADT vector to create pBADT-RboC-YFP, pBADT-RboD-YFP, and pBADT-RboE-YFP (*Figure 5*). As described in Materials and

Methods, NEB5α was used as a maintenance cell line to construct the plasmids, which were then transformed into *C. necator*. RboC-YFP, RboD-YFP, and RboE-YFP were cloned into a pBADT vector, and restriction digestion was used to confirm successful cloning (*Figure 10*). Once confirmed, plasmids were transformed into WT *C. necator* and conformational digestion was attempted numerous times in *C. necator* post-transformation. Due to difficulties in *C. necator* plasmid isolation (see 4.1.2.2 *C. necator* Plasmid Isolation Setback) only pBADT-RboE-YFP was confirmed (*Figure 11*) which casts some uncertainty on their results.

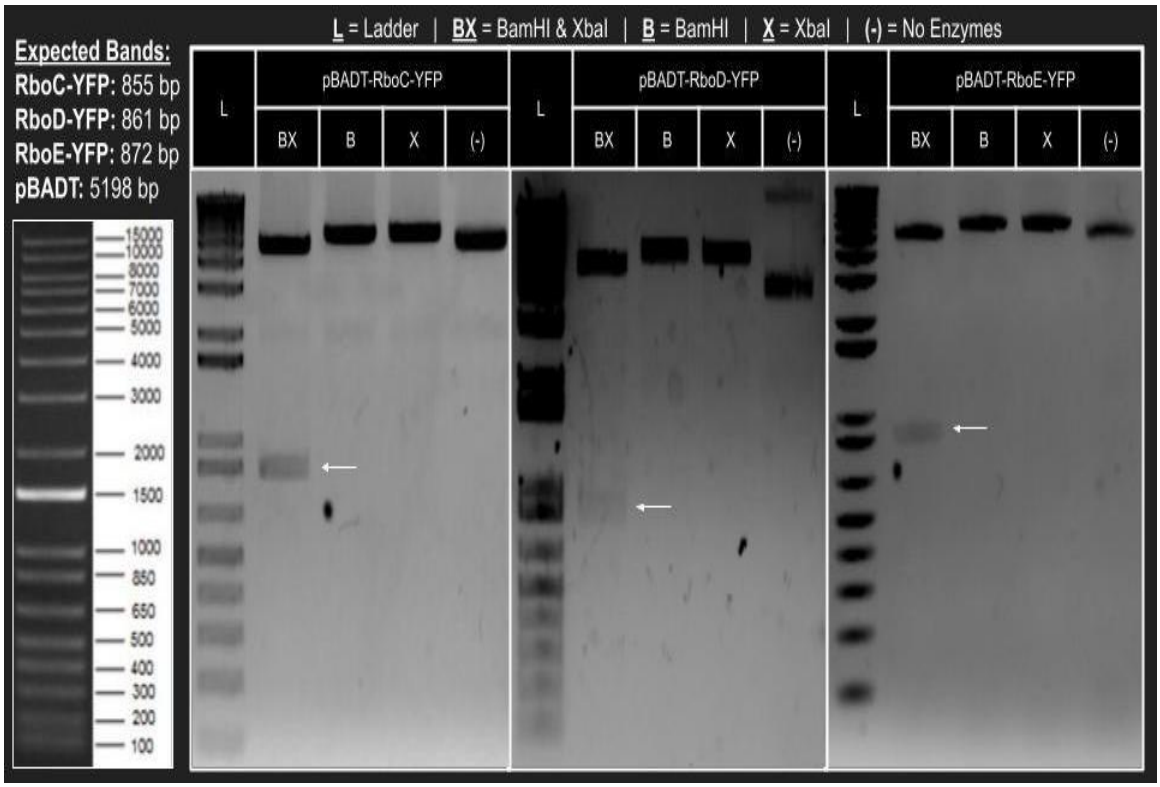

Figure 10: Conformational digest of pBADT-RboS-YFP plasmids isolated from NEB5α using BamHI and XbaI. White arrows indicate insert dropout. Any cryptic bands should be disregarded (see 4.1.2.1 Cryptic Bands Setback).

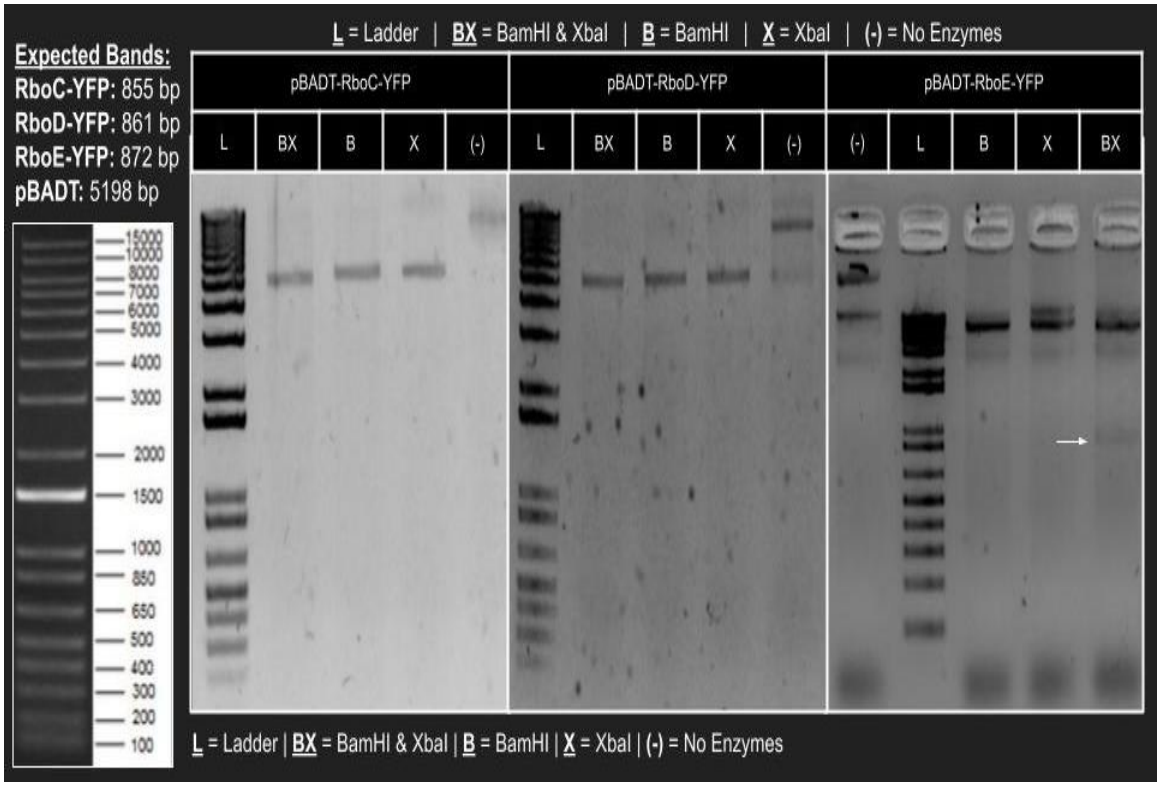

Figure 11: Representative image of multiple conformational digest (using BamHI and XbaI) attempts of pBADT-RboS-YFP plasmids isolated from *C. necator*. pBADT-RboE-YFP was only confirmed once despite numerous attempts. White arrow indicates insert dropout. Any cryptic bands should be disregarded (see 4.1.2.1 Cryptic Bands Setback).

4.1.1.2 pBADT-RboS-phaC Cloning

RboS-phaC inserts were cloned into a pBADT vector to create pBADT-RboC-phaC, pBADT-RboD-phaC, and pBADT-RboE-phaC (*Figure 6*). As described in Materials and Methods, NEB5α was used as a maintenance cell line to construct the plasmids, which were then transformed into ΔphaC *C. necator*. RboC-YFP, RboD-YFP, and RboE-YFP were cloned into a pBADT vector, and restriction digestion was used to confirm successful cloning (*Figure 12*). Once confirmed, plasmids were transformed into ΔphaC *C. necator*. Fortunately, a new Qiagen miniprep kit (Cat# 27104) was found to be successful at plasmid isolation from *C. necator*, and plasmids were confirmed post *C. necator* transformation (*Figure 13*).

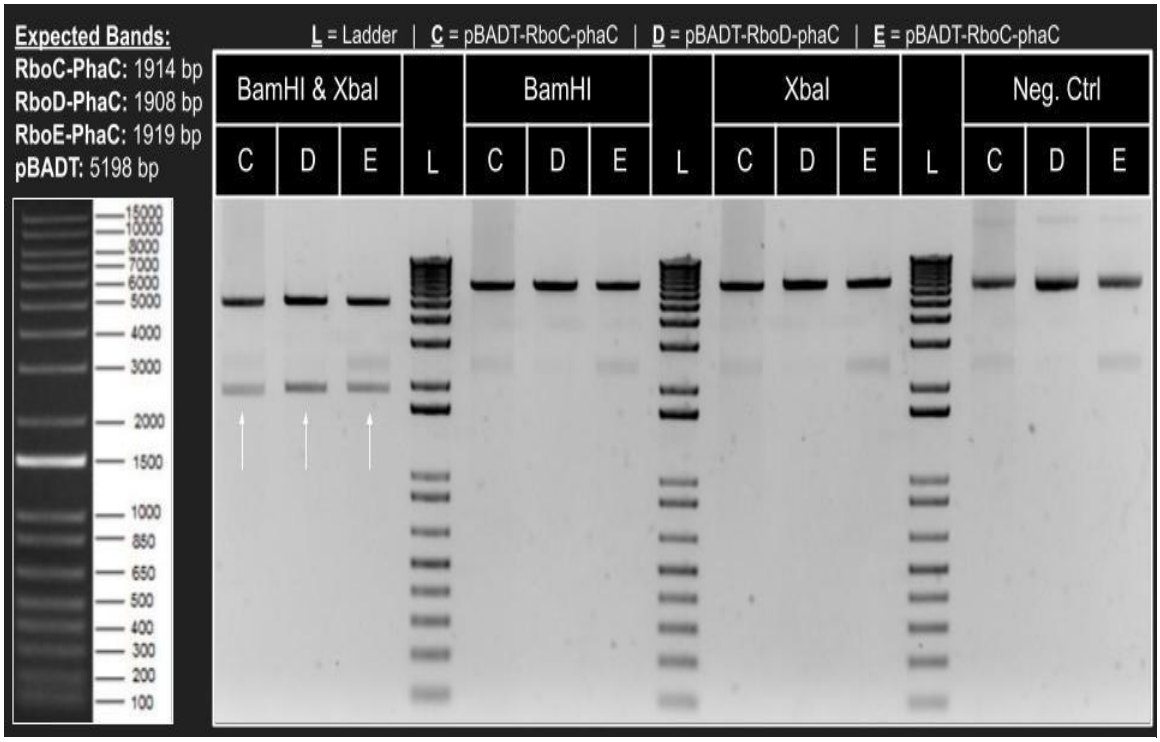

Figure 12: Conformational digest of pBADT-RboS-phaC plasmids from NEB5α using BamHI and XbaI. White arrows indicate insert dropout. Any cryptic bands should be disregarded (see 4.1.2.1 Cryptic Bands Setback).

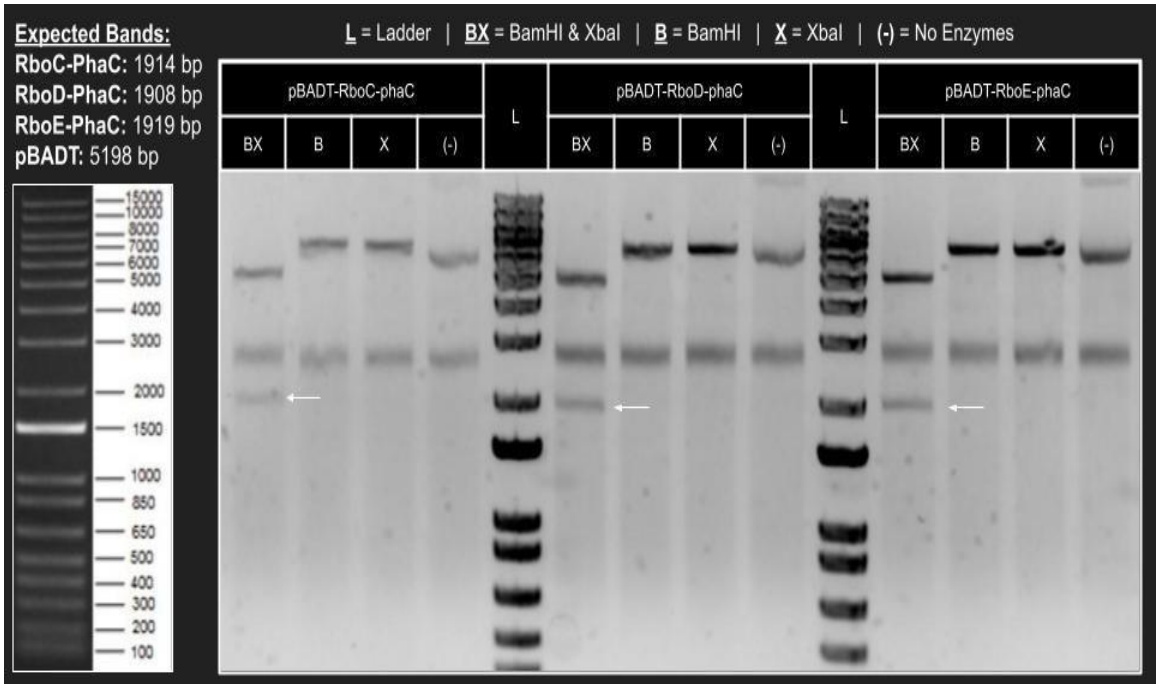

Figure 13: Conformational digest of pBADT-RboS-phaC plasmids from ΔphaC *C. necator* using BamHI and XbaI. White arrows indicate insert dropout. Any cryptic bands should be disregarded (see 4.1.2.1 Cryptic Bands Setback).

4.1.2 Cloning Setbacks

Cloning encountered two major setbacks, the first being the appearance of cryptic bands which were initially thought to be contamination. The second setback was difficulties encountered during plasmid isolation of *C. necator*. These setbacks will be addressed first before moving to the cloning results of the plasmid constructs used in this thesis.

4.1.2.1 Cryptic Bands Setback

A significant setback was caused by cryptic bands periodically appearing on agarose gels, which was initially thought to be contamination. Due to this concern, the cryptic bands were heavily investigated to ensure that cloning had properly been conducted. The bands appeared in plasmids isolated in both NEB5α and *C. necator*, and are therefore not organism specific. New kits and reagents were used, plasmids were gel excised and re-transformed, and PCR clean-up kits were conducted to no avail, indicating that contamination was not the source of the bands. To further indicate this, the bands are not consistent and would shift based on the size of the isolated plasmid (*Figure 16* & *Figure 17*), which indicates a correlation between the cryptic bands and the isolated plasmid.

Research suggested that the plasmids may have been permanently deformed due to harsh alkaline conditions, creating cryptic bands resistant to restriction enzymes but susceptible to T5 exonuclease treatment.[67] T5 exonuclease from NEB (CAT# M0363) was used on the plasmids following manufacturers protocol, which initially had success on multiple different plasmids (*Figure 14*). Plasmids were re-transformed into NEB5α, colonies were picked and grown overnight in LB, and half the culture was glycerol stocked while the other half was used for plasmid isolation. Plasmids isolated from the cultures directly after re-transformation contained no cryptic band, suggesting that the issue was

resolved. However, when the glycerol stock was later used to isolate more plasmid, the cryptic bands spontaneously appeared again (*Figure 15*). Furthermore, glycerol stocking was not the only storage medium in which cryptic bands would spontaneously appear. A plasmid stock stored at -20°C in water was confirmed to have no cryptic bands, however, cryptic bands reappeared spontaneously when checked at a later date (*Figure 16*). Another interesting property of the bands is that they sometimes disappeared on agarose gels when the gels are run for a longer period of time (*Figure 18*).

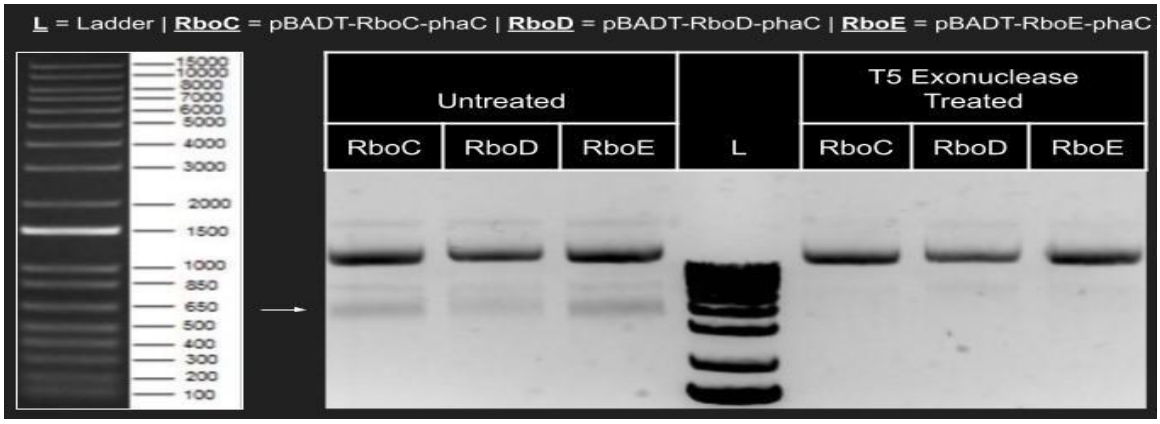

Figure 14: pBADT-RboS-phaC plasmids isolated from NEB5α and treated with T5 exonuclease. Cryptic bands are not apparent with T5 Exonuclease treatment.

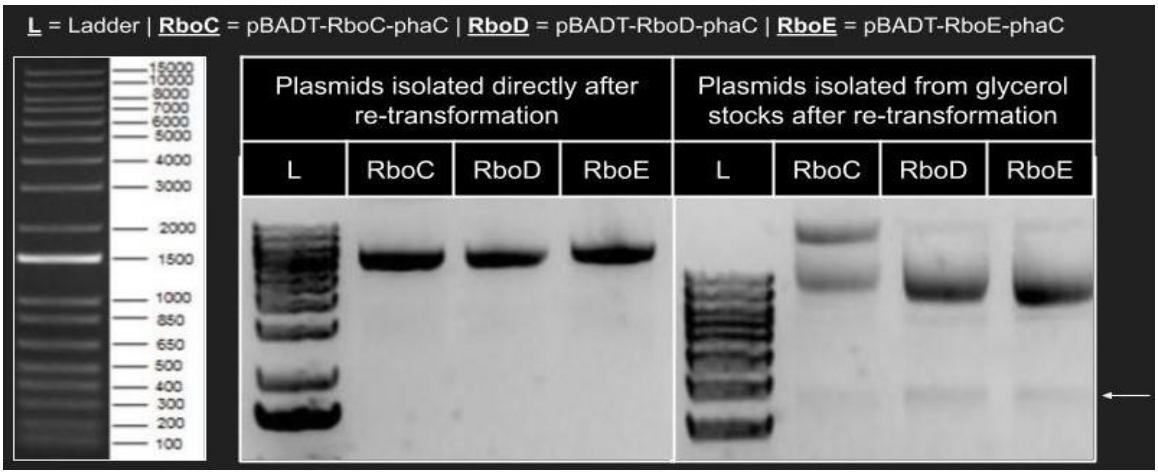

Figure 15: pBADT-RboS-phaC plasmids were treated with T5 exonuclease and re-transformed into NEB5α. Half the culture was then glycerol stocked, and the other half was used for plasmid isolation. Untreated plasmids isolated directly after re-transformation contain no cryptic bands. Untreated plasmids isolated from the glycerol stocks contain cryptic bands. White arrow indicates the location of the cryptic bands.

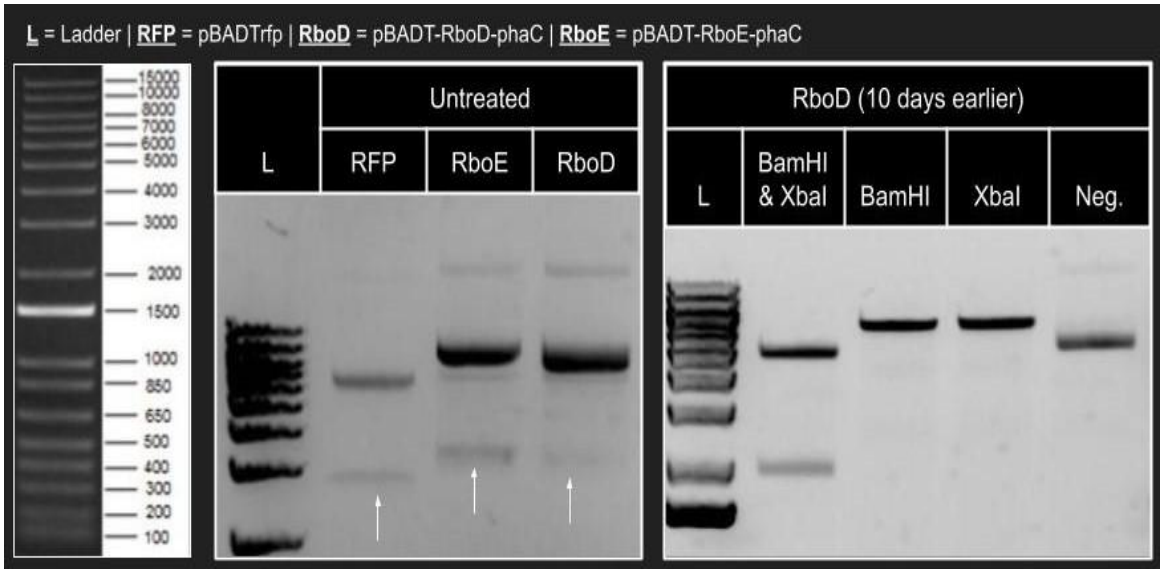

Figure 16: An experiment to observe a shift in the cryptic band sizes between pBADTrfp plasmids (a significantly smaller plasmid of 5927 bp) and pBADT-RboE-phaC plasmids (a significantly larger plasmid of 7717 bp). White arrow indicates cryptic band location. Cryptic bands are significantly smaller in pBADTrfp compared to pBADT-RboE-phaC. The pBADT-RboD-phaC lane was intended to be used as a negative control, as 10 days earlier the plasmid stock contained no cryptic bands. The plasmid was stored in sterile water at -20°C but was otherwise untouched. Cryptic bands spontaneously appeared during this experiment.

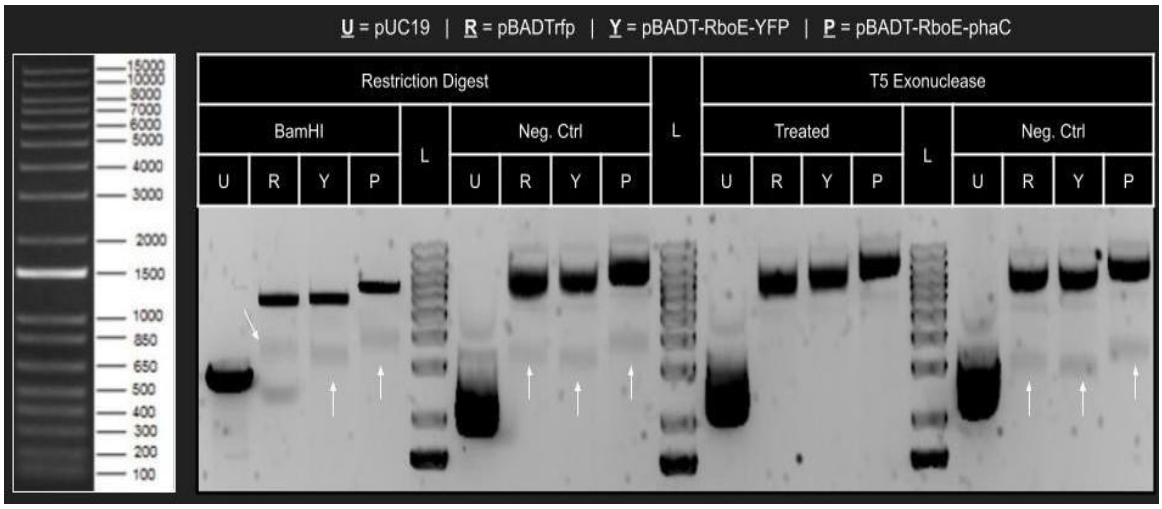

Figure 17: Investigating the properties of the cryptic bands in multiple conditions. White arrows indicate cryptic bands. Multiple plasmids were treated with BamHI and T5 exonuclease. Cryptic bands were resistant to restriction enzymes but were susceptible to T5 exonuclease. Cryptic bands only appear in plasmids containing a pBADT vector. The size of the cryptic bands is dependent on the plasmid, with the cryptic band in pBADT-RboE-phaC being consistently the highest band, followed by pBADTrfp, and lastly by pBADT-RboE-YFP.

In summary, the cryptic bands appear independent of reagents, kits, or cell lines used. Cryptic bands only appear in plasmids with a pBADT vector, and their sizes are dependent on the plasmid. The bands spontaneously appear in different storage conditions, both from glycerol cultures at -80°C and plasmid stocks in water stored at -20°C. Lastly, the bands are resistant to restriction enzymes but are susceptible to T5 exonuclease treatment. Considering that T5 exonuclease also contains single-stranded endonuclease activity, the cryptic bands are most likely due to the plasmid constructs having a natural tendency to separate into a single-stranded configuration and should be dismissed when analyzing cloning results.

4.1.2.2 C. necator Plasmid Isolation Setback

Plasmid isolation from *C. necator* often failed or would provide ambiguous results, making plasmid confirmation difficult. Different kits were used as well as homemade alkaline lysis (see Materials and Methods) was conducted, but plasmid isolation would routinely fail regardless of method used. Even when plasmid isolation was successful the results were often ambiguous. When successful, plasmids isolated from *C. necator* were digested for restriction confirmation and would show vector bands that would have a significant shift in double digested condition, indicating a drop out. However, the dropout itself would not be visible (*Figure 18*). The cause of this is unknown and consistently occurred with plasmids isolated from *C. necator*. Some plasmids were therefore not fully confirmed post-transformation in *C. necator*. Later, during the cloning of pBADT-RboS-phaC plasmid constructs, a new Qiagen kit was attempted (CAT# 27104) which was successful in isolating plasmids from *C. necator*. Due to this, some pBADT-RboS-YFP constructs were not confirmed through restriction digestion in *C. necator* post-

transformation, but all pBADT-RboS-phaC plasmid constructs were confirmed in *C. necator* post-transformation.

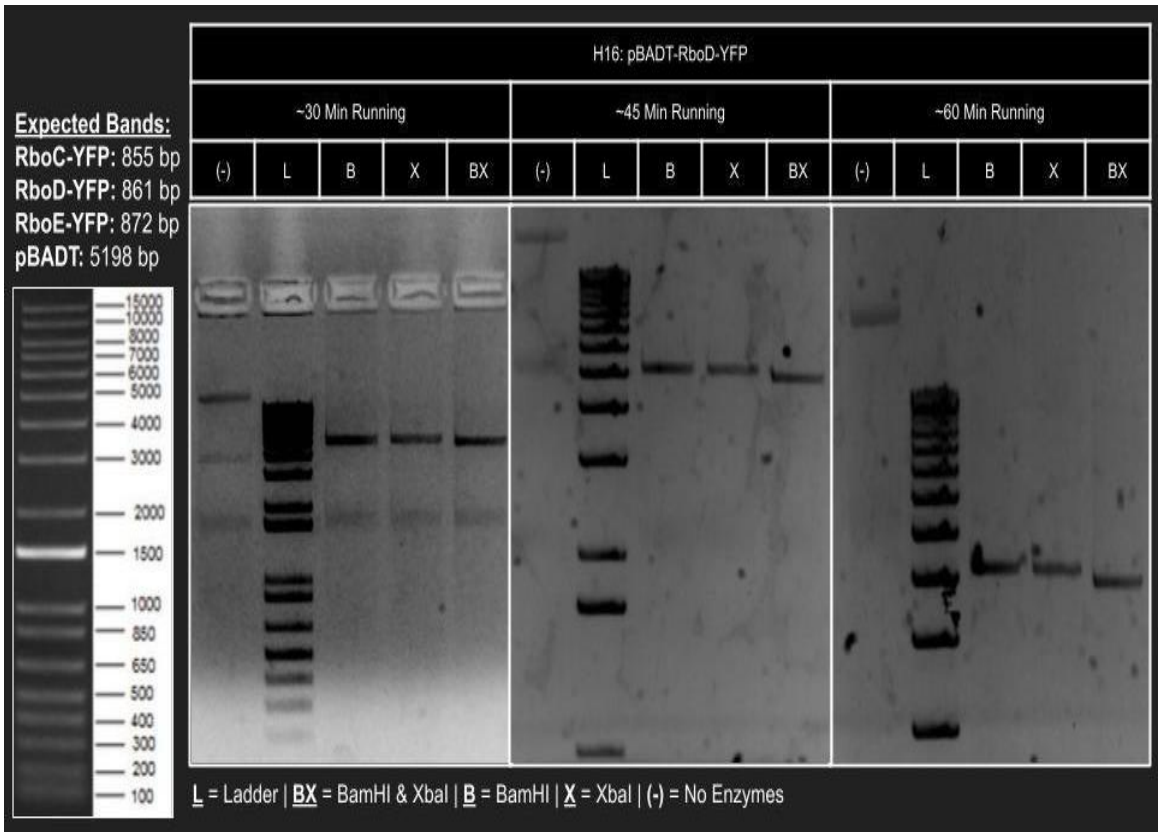

Figure 18: A representative image of plasmids isolated from *C. necator*. pBADT-RboD-YFP was isolated and digested with BamHI and XbaI before gel electrophoresis. Images were taken at 30, 45, and 60 minutes. Both enzymes were able to cut the plasmid, and the double digested cryptic band is visibly smaller (most apparent at the 60 minute mark). Despite this indicating a dropout for the double digested lane, no dropout was ever visible at any point. Cryptic bands can be seen at the 30 minute mark (~1750 bp), but disappear in later images.

4.2 Riboswitch Functionality using Fluorescence Reporter Genes

The degree of functionality in the riboswitches can vary based on the model organism,[20] and it was therefore important to first demonstrate that the riboswitches would be functional *C. necator*. For this, YFP was initially used to determine riboswitch functionality in the model organism, through both qualitative and quantitative methods.

4.2.1 Qualitative Imaging

Before testing any of the riboswitches, the pBADT vector needed to be demonstrated as functional in *C. necator*. Specifically, L-arabinose was needed to be shown as permeable into *C. necator*, and that the pBADT vector's arabinose inducible promoter would function properly. For this, the pBADTrfp plasmid was transformed into wildtype (WT) *C. necator* and grown in the presence of L-arabinose for FACS. Fortunately, FACS was unnecessary, as the cultures generated a significantly visible red colour when grown under inducible conditions (*Figure 19*). The arabinose inducible promotor of pBADTrfp is directly controlling the expression of RFP. The red colour of the cultures grown in the presence of L-arabinose demonstrates the expression of RFP controlled by the arabinose inducible promotor, and therefore the functionality of pBADT's arabinose inducible promotor in *C. necator*.

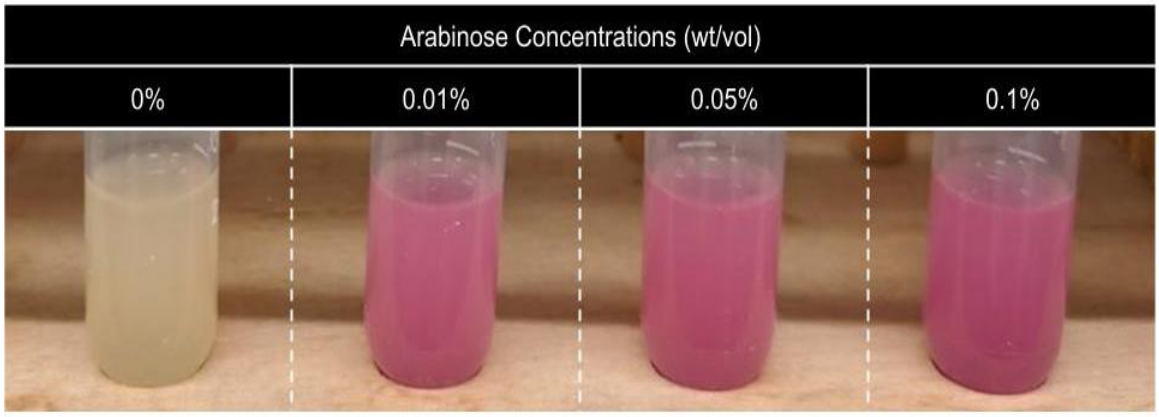

Figure 19: WT *C. necator* transformed with pBADTrfp grown in LB containing kanamycin and L-arabinose at various concentrations, grown overnight at 30°C and 250 rpm. Red color is apparent in all growth conditions excluding the negative control.

With the pBADT vector demonstrated to be functional, riboswitch functionality was then explored. For this, WT *C. necator* (acting as a true negative control) was grown in the presence of 0.01% (wt/vol) L-arabinose and 2 mM theophylline. *C. necator*

transformed with one of the pBADT-RboS-YFP variants were grown in the absence of L-arabinose and theophylline, as well as in the presence of 0.01% (wt/vol) L-arabinose and/or 2 mM theophylline. Cultures were then subjected to visual examination as well as fluorescent imaging. Similar to pBADTrfp, there was a visible yellow colour in *C. necator* transformed with the pBADT-RboE-YFP when grown in the presence of both L-arabinose and theophylline, however, pBADT-RboC-YFP and pBADT-RboD-YFP generated no such visible colour change. Although there was a visible colour change only apparent in *C. necator* pBADT-RboE-YFP plasmid, there could have been some activity in the other riboswitch variants that were not detectable through visual examination. To explore this possibility the Amersham Imager 600 was found to be able to detect fluorescent activity in YFP and was used for increased sensitivity for qualitative images. Confirming the visual results, the only condition that expressed fluorescent activity was *C. necator* pBADT-RboE-YFP grown in the presence of both L-arabinose and theophylline (*Figure 20*). In the pBADT-RboS-YFP constructs the expression of YFP is controlled by both the arabinose inducible promotor and the riboswitch variants. The arabinose inducible promotor is controlling the transcription of the RboS-YFP mRNA, and the translation of the RboS-YFP mRNA is controlled by the riboswitch variants. The observed fluorescent activity is only demonstrated (through both visual means and through imaging) in the pBADT-RboE-YFP construct, and only when grown in the presence of both L-arabinose and theophylline. This demonstrates that both the arabinose inducible promotor and, more importantly, the RboE variant is functional in *C. necator*.

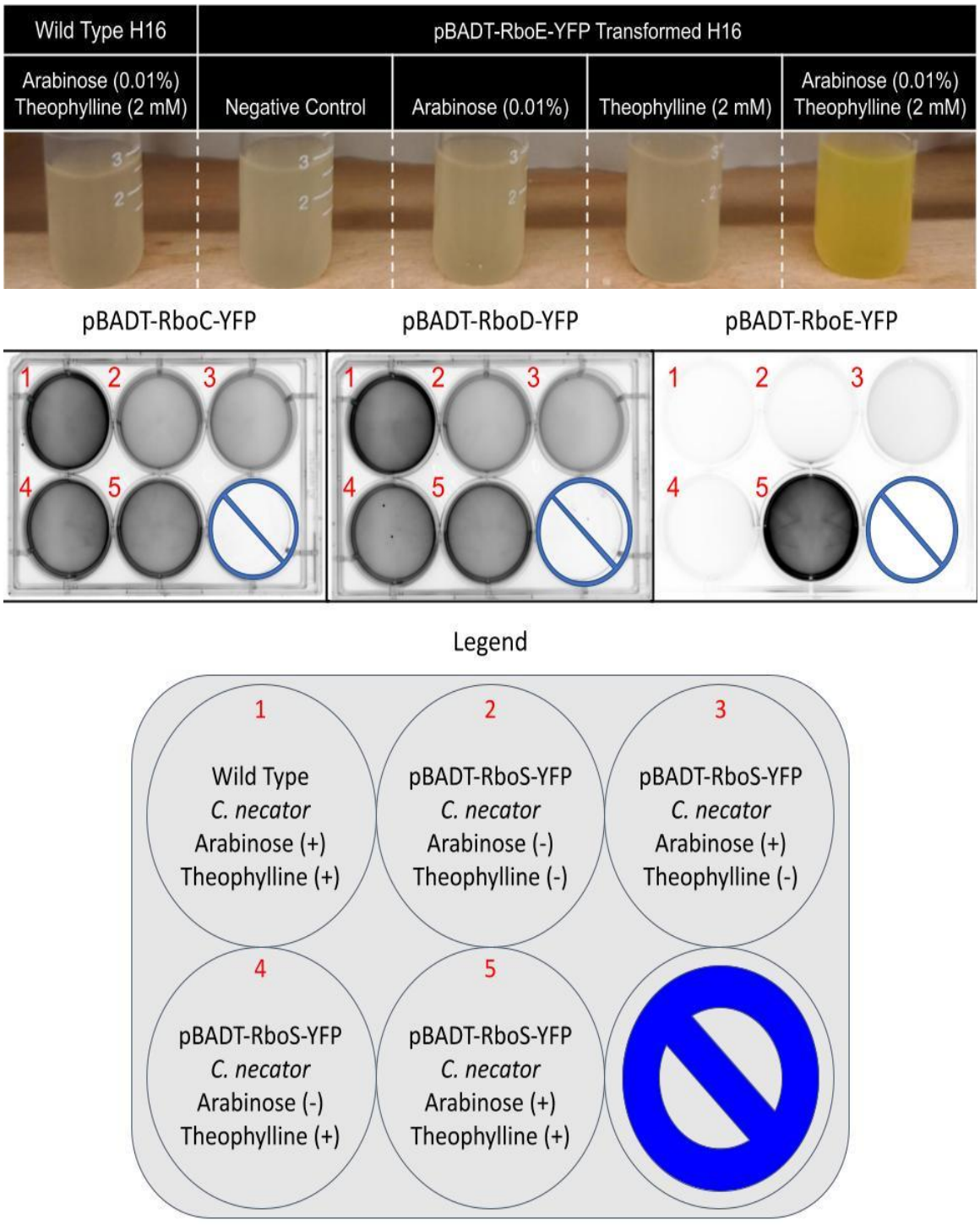

Figure 20: Cultures were grown in 15 mL culture tubes overnight in LB containing kanamycin at 30°C and 250 rpm. Cultures were visually investigated and poured into 6 well plates for imaging using Amersham Imager 600. Images were taken through a 605BP40 filter after exposure to a wavelength of 520 nm for 0.2 seconds each. The image for pBADT-RboE-YFP appears faded due to image saturation from fluorescent activity in the L-arabinose and theophylline condition, and is not due to a different exposure time.

4.2.2 Quantifiable Fluorescent Results

Although the qualitative results strongly suggest that the only riboswitch variant functional in *C. necator* is RboE, all riboswitches were examined through FACS for increased sensitivity and to generate quantitative results. FACS is a significantly more sensitive measurement compared to the qualitative methods previously deployed and may be able to detect fluorescent activity that visual and imaging analysis was unable to detect. Furthermore, FACS allows for a quantifiable determination of the degree of increased functionality that RboE has compared to RboC and RboD, as well as to characterize the exact nature of that functionality (such as any leaky expression that may exist). For this, WT *C. necator* (acting as a true negative control) and WT *C. necator* transformed with one of the pBADT-RboS-YFP variants were grown in the absence of L-arabinose and theophylline, as well as in the presence of 0.01% (wt/vol) L-arabinose and/or 2 mM theophylline. FACS was performed as described in the Materials and Methods. RboE was again confirmed to be the only functional riboswitch (*Figure 21* & *Table 2*).

RboE was demonstrated as the only functional riboswitch through visual results, qualitative imaging, and FACS. This, however, could be disputed, as conformation of pBADT-RboC-YFP and pBADT-RboD-YFP post *C. necator* transformation was ambiguous, and their lack of fluorescent activity could be attributed as a cloning failure. Despite this, RboE's functionality was significantly robust, with low levels of leaky expression and high levels of induced expression.

Table 2: Percentage of florescent cells determined by FACS post gating.

	Neg. Control	Arabinose	Theophylline	Arabinose & Theophylline
WT	0.001%	0%	0%	0%
RboC	0%	0%	0%	0%
RboD	0%	0%	0%	0%
RboE	0%	0.009%	0%	74.231%

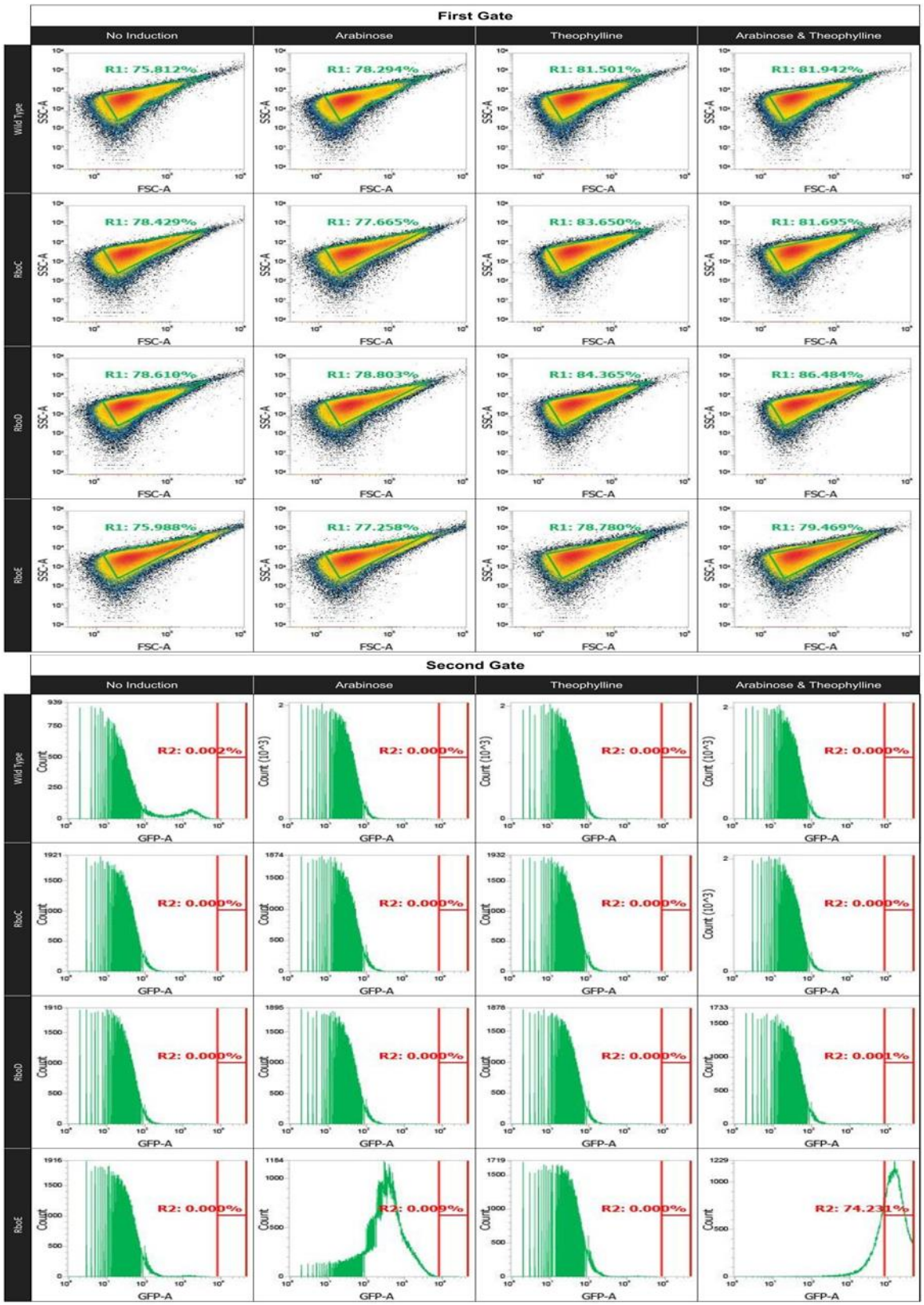

Figure 21: FACS results of WT *C. necator* as well as *C. necator* transformed with pBADT-RboC-YFP, pBADT-RboC-YFP, or pBADT-RboE-YFP.

4.3 Riboswitch Functionality for Industrial Application

Riboswitch functionality for industrial application was explored simultaneously through western blotting and gas chromatography. This required significant optimization for both gas chromatography and *C. necator* growth conditions. Gas chromatography on PHB standards was first examined to ensure reliable gas chromatography settings for PHB detection and quantification. Preliminary results on PHB extracted from *C. necator* indicated that L-arabinose and/or theophylline may impact the metabolism of PHB and optimization of growth conditions was therefore also performed. Once both gas chromatography and growth conditions were optimized, phaC expression was examined through western blotting and PHB production was examined through gas chromatography.

4.3.1 Analysis of PHB Standard

Before PHB production in *C. necator* was examined, demonstrating reliable PHB standards and reference samples was needed to determine appropriate gas chromatography settings. PHB standards were prepared as described in Materials and Methods, and samples were analyzed through gas chromatography numerous times through different settings until reliable peaks were detected at around the 2.7 minute mark. Once proper settings (as described in Materials and Methods) were determined, standards were analyzed in triplicate to demonstrate reliability of PHB detection by GC (*Figure 22* & *Table 3*).

Table 3: The value of the area under the peak for all standard samples. The standard was conducted in triplicate, and three separate readings were taken for each replicate.

		Area [µV.Min]		
PHB	**Replicate**	**Reading 1**	**Reading 2**	**Reading 3**
0 µg	**1**	0.1	0.1	0.5
	2	0	1	0.1
	3	0.2	0.3	0.2
15 µg	**1**	4.5	5.7	6.2
	2	7.2	6.7	6.7
	3	8.5	8.3	8.4
30 µg	**1**	10.9	10.7	11.4
	2	16.4	15.4	15.8
	3	12	11.2	11.9
45 µg	**1**	18.7	19.4	20.5
	2	23.2	24.1	25.3
	3	21.7	21.8	23.2
60 µg	**1**	26.2	25.8	24.2
	2	25	24.7	27
	3	29.6	30.5	30.1
75 µg	**1**	31.6	32.2	33.6
	2	33.7	33.9	35.3
	3	37.2	37.2	37
90 µg	**1**	37.6	40.0	37.3
	2	42.6	42.1	44.1
	3	45.8	47.3	47.2

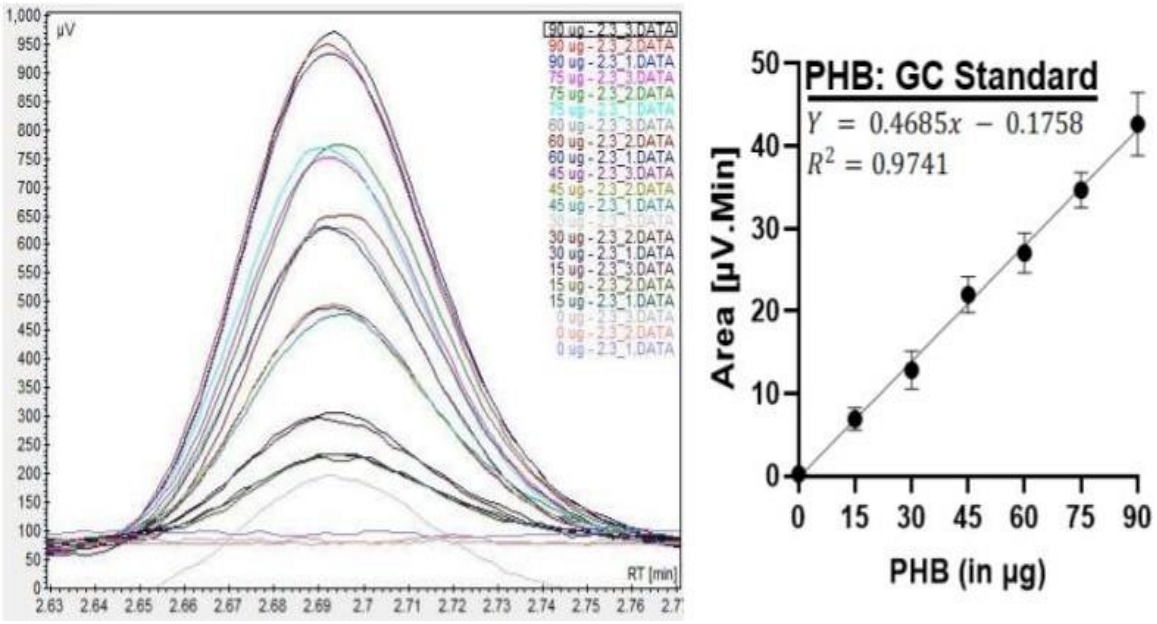

Figure 22: Representative chromatogram of PHB standards done in triplicate, alongside quantification of standards and standard curve.

4.3.2 Growth Condition Optimization

With gas chromatography settings optimized, an experiment involving ΔphaC *C. necator* pBADT-RboE-phaC was performed to set up the pipeline for PHB extraction from *C. necator*. pBADT-RboE-phaC was chosen as it was demonstrated to be the only reliable riboswitch from the fluorescent results. For this, WT *C. necator* and ΔphaC *C. necator* containing pBADT-RboE-phaC were grown in the presence and absence of 0.01% (wt/vol) L-arabinose and 2 mM theophylline, and were subjected to both western blotting and gas chromatography as described in Materials and Methods. Western blotting demonstrated robust phaC expression in pBADT-RboE-phaC, however for both WT *C. necator* and ΔphaC *C. necator* pBADT-RboE-phaC the best PHB production occurred in the L-arabinose and theophylline absent conditions (*Figure 23* & *Table 4*).

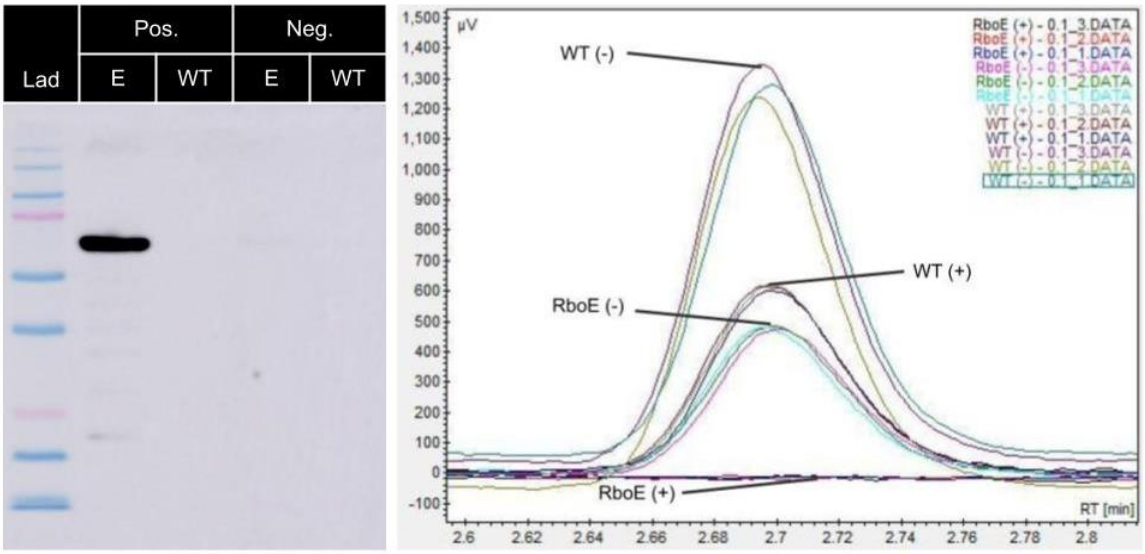

Figure 23: Preliminary results investigating phaC and PHB production in ΔphaC *C. necator* controlled by RboE. "Pos." condition indicates growth in both 0.01% (wt/vol) L-arabinose and 2 mM theophylline, "Neg." condition indicates growth in the absence of L-arabinose and theophylline.

Table 4: The value of the area under the peak for gas chromatography of the preliminary results. PHB production was determined using the standard curve from 4.3.1 Analysis of PHB Standard.

Culture	Growth Condition	Average Area[µV.Min]	PHB Production
pBADT-RboE-phaC	Arabinose and Theophylline	0.63	1.73 µg
	Negative Control	25.06	55.02 µg
WT C. necator	Arabinose and Theophylline	32.83	70.46 µg
	Negative Control	66.33	141.96 µg

This preliminary experiment was intended to determine a pipeline from growth and induction of the bacteria to PHB extraction and analysis. Establishing this pipeline (as described in Materials and Methods) was necessary to expose any unexpected issues or experimental errors that may occur. Two experimental errors were identified. One error is that a reference sample was not used to confirm the peak location of PHB. The other error

was that the induction growth conditions contained both L-arabinose and theophylline, with no induction conditions containing only one of the inducers. More importantly, the results suggested an unexpected issue with one or both of the inducers. The best PHB production occurred in the L-arabinose and theophylline absent conditions, raising a concern that L-arabinose and/or theophylline may impact the metabolism of *C. necator* and interfere with PHB production. Due to this concern, the impact of L-arabinose and/or theophylline was investigated.

The first avenue investigated explored the use of D-arabinose. If L-arabinose is the cause for the interference in PHB production, then D-arabinose may circumvent the issue. However, before PHB production could be investigated, demonstrating that the pBADT arabinose promoter could be induced by D-arabinose was required. Western blotting of pBADT-RboE-phaC ΔphaC *C. necator* grown in the presence of theophylline, and/or L/D-arabinose was investigated as described in Materials and Methods. Unfortunately, D-arabinose was incapable of inducing the pBADT arabinose promoter and was therefore determined to be unusable (*Figure 24*).

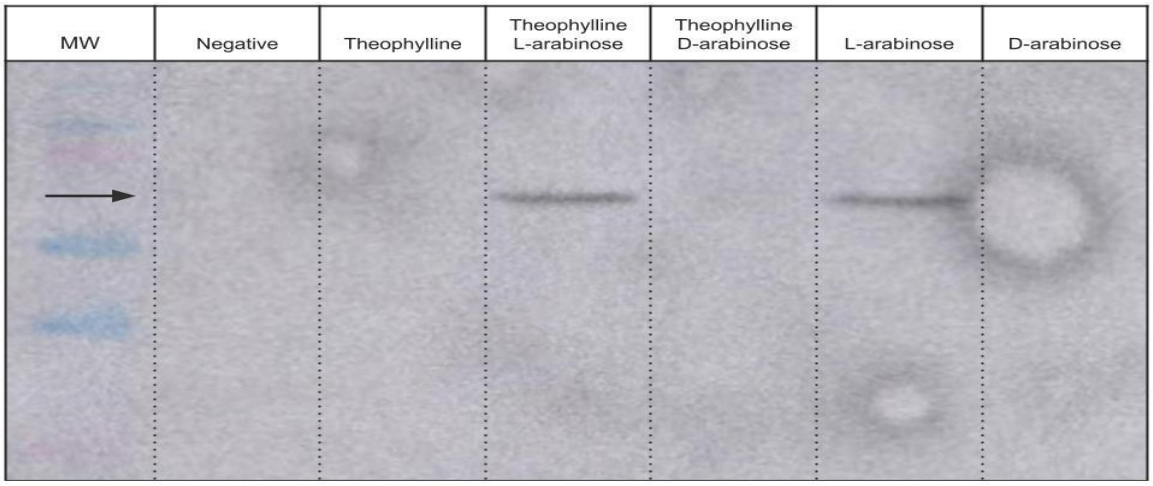

Figure 24: Western blotting for phaC production in pBADT-RboE-phaC ΔphaC *C. necator*, grown in presence of theophylline and/or L/D-arabinose. The black arrow indicates phaC protein size.

With L-arabinose as the only available option, optimization moved to investigate the ideal concentrations for both L-arabinose and theophylline, specifically looking for concentrations that would not (or would have little) interference on PHB production while inducing the pBADT arabinose promoter and theophylline riboswitch. To determine the impact of L-arabinose and theophylline on native PHB metabolism, WT *C. necator* was grown in various concentrations of both L-arabinose and theophylline before being analyzed through gas chromatography as described in Materials and Methods. A reference sample containing 25 µg of PHB and a blank was used alongside the experiment to determine proper extraction and peak identification (*Figure 25* & *Table 5*).

Table 5: The value of the area under the peak for gas chromatography of the optimization of L-arabinose and theophylline concentration. PHB production was determined using the standard curve from 4.3.1 Analysis of PHB Standard.

Growth Condition		Average Area [µV.Min]	PHB Production
Theophylline Concentration	Arabinose Concentration (wt/vol)		
2 mM	0.001%	31.57	67.75 µg
0 mM	0%	23.73	51.03 µg
2 mM	0%	23.97	51.53 µg
	0.0025%	31.90	68.46 µg
	0.005%	28.17	60.50 µg
	0.0075%	29.77	63.91 µg
0 mM	0.001%	27.07	58.15 µg
0.5 mM		27.60	59.29 µg
1 mM		33.00	70.81 µg
1.5 mM		30.80	66.12 µg
PHB Reference (25 µg)		*10.70*	*23.21 µg*
Blank		*0.57*	*1.58 µg*

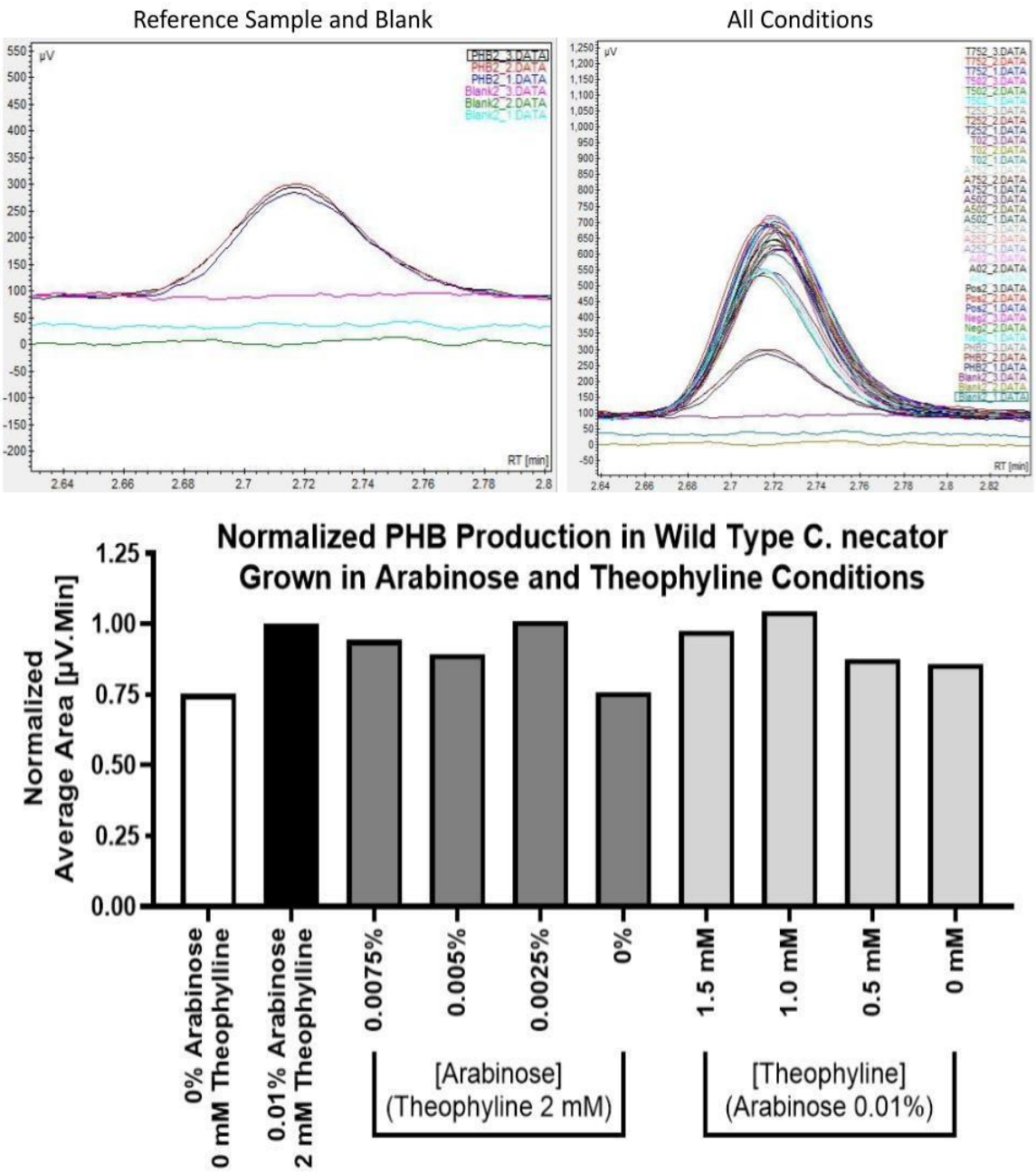

Figure 25: WT *C. necator* growth conditions used the concentrations from fluorescence experiments (0.01% (wt/vol) L-arabinose and 2 mM theophylline) as a start point. Keeping one of the inducer (arabinose or theophylline) concentrations constant, a decreasing concentration gradient of the other was examined. Chromatograph of the reference sample and blank, as well as all growth conditions, are shown. The area under the peaks were analyzed and normalized to the initial 0.01% (wt/vol) L-arabinose and 2 mM theophylline growth condition for graphical representation.

Results from this experiment are vastly different than the preliminary results. Preliminary results suggest that L-arabinose and/or theophylline interfere with PHB production (*Figure 23* & *Table 4*), however, this experiment would indicate the opposite. PHB production of WT *C. necator* grown in the highest concentration of both inducers (67.75 µg) is more than the PHB produced when grown in the absence of both inducers (51.03 µg), in the absence of just L-arabinose (58.15 µg), and in the absence of just theophylline (51.53 µg). This indicates that both L-arabinose and theophylline enhance PHB production rather than interfere with it, contradicting the preliminary results. Furthermore, the preliminary results show massive changes in PHB production, with WT *C. necator* producing double the PHB when grown in the absence of both inducers (141.96 µg) compared to growth in presence of both inducers (70.46 µg). This is vastly different from the results shown in this experiment, as PHB production is roughly between 50 µg to 70 µg for all conditions. There also doesn't appear to be a reliable trend based on inducer concentration. Decreasing the concentration of one inducer while keeping the other constant doesn't demonstrate a consistent impact on PHB production. For L-arabinose, PHB production decreases with concentration until 0.0025%, where production suddenly increases. The same is true for theophylline, PHB production also decreases with concentration until 1 mM, where production increases again. Even with these random increases, the observed changes in the different concentrations are minor (within 50 µg to 70 µg) when compared to the major changes observed in the preliminary results.

Because these results contradict the preliminary results, the fact that observed increases and decreases are not nearly as obvious as the preliminary results suggest they should be, and because these results do not demonstrate a reliable trend, it was determined

that the preliminary results were unreliable, and any observed changes in PHB production for this experiment are most likely background noise. Therefore, L-arabinose and theophylline likely do not have a significant impact on PHB production. Although L-arabinose and theophylline may not significantly impact PHB production, they still could be optimized for induction. To determine this, pBADT-RboE-phaC ΔphaC *C. necator* was grown in identical conditions, and western blotting was used to determine the impact on induction (*Figure 26*).

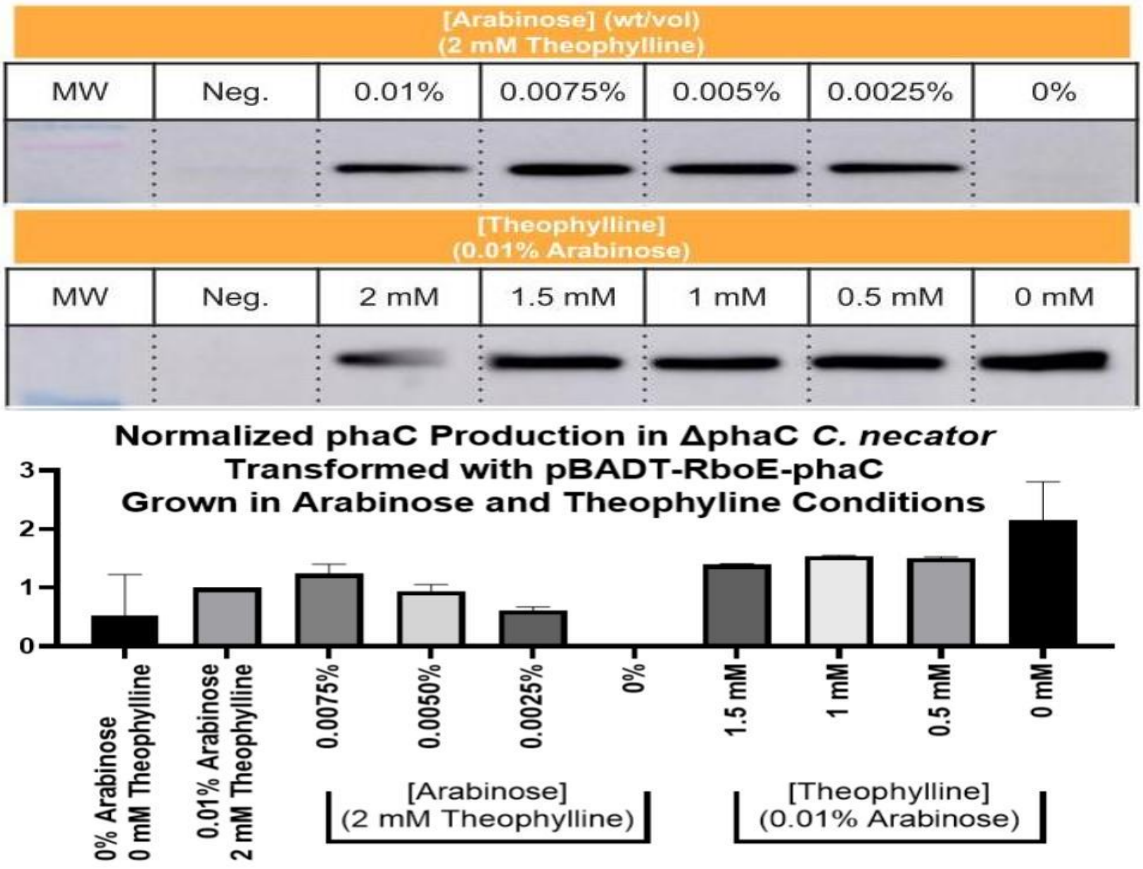

Figure 26: pBADT-RboE-phaC ΔphaC *C. necator* growth conditions used the concentrations from fluorescence experiments (0.01% (wt/vol) L-arabinose and 2 mM theophylline) as a start point. Keeping one of the inducer (arabinose or theophylline) concentrations constant, a decreasing concentration gradient of the other was examined. Lysates were analyzed in technical duplicate. Representative western blot is shown, alongside a graphical representation of western blot data, normalized to ponceau staining and to the initial 0.01% (wt/vol) L-arabinose and 2 mM theophylline growth condition. Error bars are from a single experiment with the lysate being western blotted twice.

Unlike gas chromatography results for PHB production, L-arabinose and theophylline concentrations appear to have an impact on induction with obvious trends. L-arabinose appears to operate better at the slightly lower 0.0075% (wt/vol) concentration and decreases consistently from that point. Theophylline was consistently better at all lower concentrations, with the theophylline absent condition producing the most phaC (despite large error margins). This result suggests that RboE is non-functional and is in direct opposition to previous FACS data. Furthermore, this confusing result will be later confirmed numerous times when analyzing the effectiveness of the different riboswitch variants in phaC production. Still, data indicates that a lower concentration of both L-arabinose and theophylline improve their ability to induce the promoter and riboswitch respectively. 0.0075% (wt/vol) L-arabinose and 1 mM theophylline was determined to be optimal concentrations based on these results and was therefore used for subsequent experiments.

4.3.3 Industrial Application of Riboswitch Variants

With optimization experiments concluded, the new L-arabinose and theophylline concentrations were used to analyze the effectiveness of all riboswitch variants for the control of phaC expression and PHB production. ΔphaC *C. necator* transformed with one of the pBADT-RboS-phaC variants were grown (in biological triplicate) in the absence of L-arabinose and theophylline, as well as in the presence of 0.0075% (wt/vol) L-arabinose and/or 1 mM theophylline, and were then analyzed through western blotting and gas chromatography to determine phaC expression and PHB production respectively, as described in Materials and Methods. In complete opposition to the fluorescent experiments, RboC and RboD were fully functional in the production of phaC, with RboE being

completely non-functional. RboC in particular had the most robust induction capabilities with the lowest leaky expression (*Figure 27*).

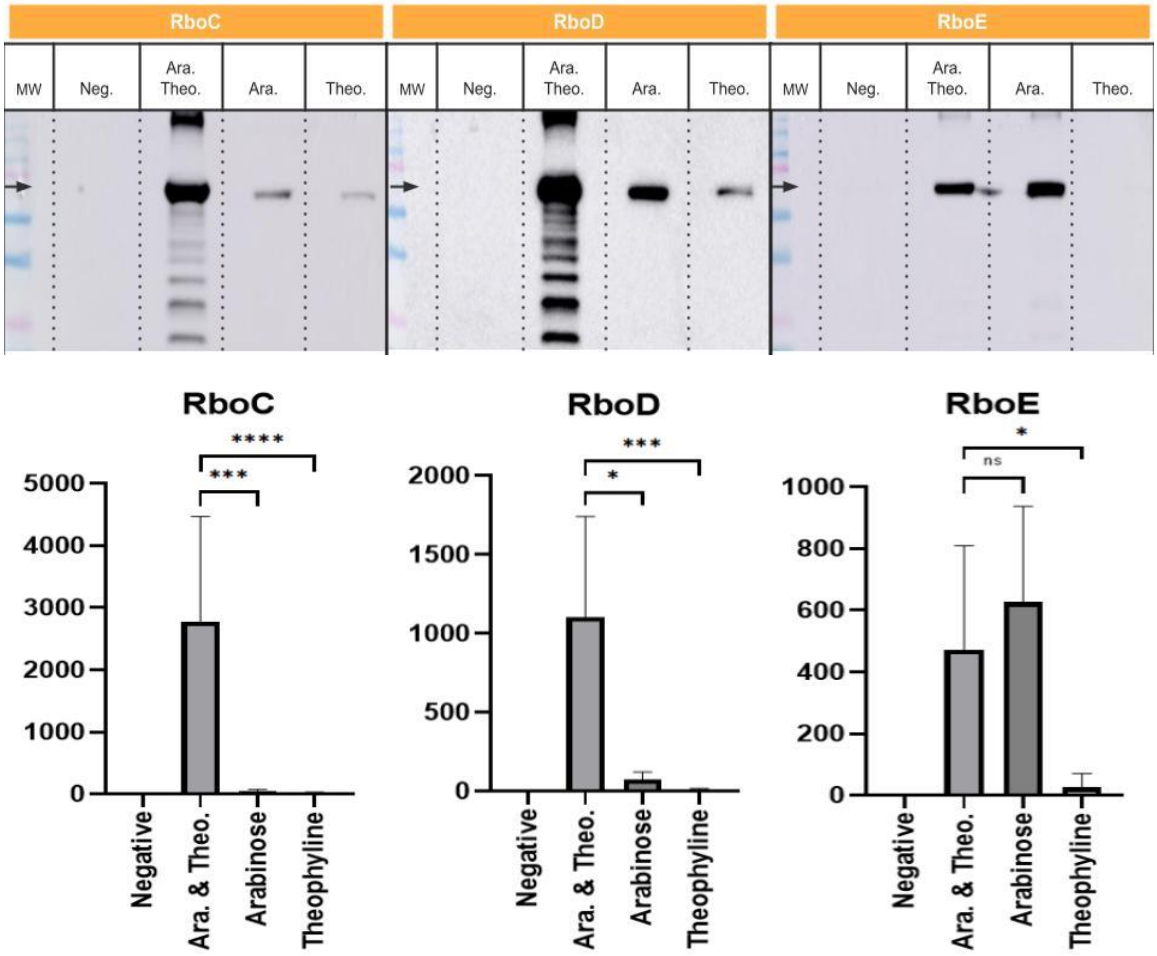

Figure 27: Western blotting for phaC production was conducted in biological triplicate. A representative western blot of all three riboswitch variants is shown alongside graphical data for biological triplicates. The black arrow indicates phaC protein size.

Although surprising, literature has previously established that alteration in the sequence surrounding a riboswitch can disrupt the riboswitch's structure, and therefore disrupt its function.[21,68] It is reasonable to suggest that YFP downstream of RboC and RboD causes them to be non-functional in *C. necator*, but when YFP is replaced with phaC, RboC and RboD become functional (with the inverse of this being true regarding RboE). It is also important to note that RboC-YFP and RboD-YFP were non-functional due to producing no

GOI upon induction, while RboE-phaC is non-functional due to the production of the GOI regardless of induction. This demonstrates a different mechanism regarding why and how loss-of-function occurs in the different riboswitches. RboC-YFP and RboD-YFP loss-of-function is most likely due to the formation of a secondary structure in which the RBS is strongly sequestered regardless of the presence of theophylline. In contrast, RboE-phaC loss-of-function is most likely due to the formation of a secondary structure in which the RBS is exposed regardless of the presence of theophylline. In both cases, the most likely cause of this is that the aptamer domain may be disrupted and unable to bind to theophylline. Another possibility is that the aptamer domain is still capable of binding to theophylline, however, the binding of theophylline is unable to cause a conformational change significant enough that the RBS becomes exposed/sequestered. As previously addressed, pBADT-RboC-YFP and pBADT-RboD-YFP were never confirmed post *C. necator* transformation, and there is always a possibility that their inability to produce YFP was due to cloning error. Even if true, RboE was confirmed through restriction digestion in both pBADT-RboE-YFP and pBADT-RboE-phaC post *C. necator* transformation and demonstrated significant functionality when controlling YFP with a significant loss-of-function when controlling phaC.

With phaC production being demonstrated with pBADT-RboC-phaC and pBADT-RboD-phaC, gas chromatography was used to determine PHB production. Despite clear phaC expression, gas chromatography was unable to detect PHB in any of the conditions for all three biological replicates. A PHB standard (consisting of 20 µg, 40 µg, 60 µg, 80 µg, and 100 µg) and blank was used alongside samples, confirming the lack of PHB production was not due to extraction or machine error (*Figure 28* & *Table 6*).

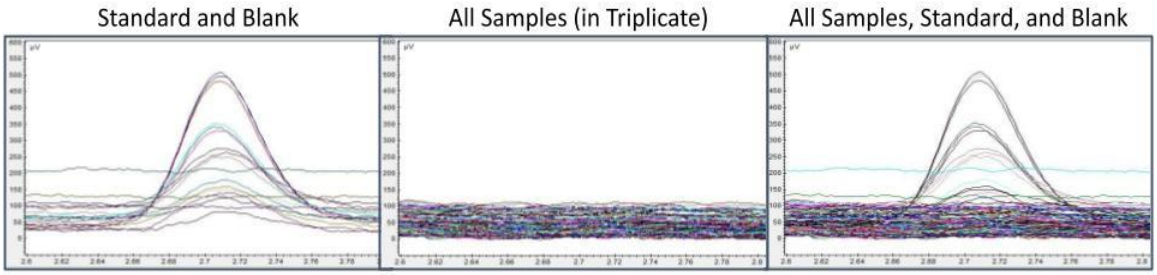

Figure 28: Chromatograph of gas chromatography results for PHB production under riboswitch control. Standards were reliable and no PHB production was demonstrated in samples.

Table 6: The value of the area under the peak for gas chromatography of PHB production controlled by all three riboswitch variants.

		Average Area[µV.Min]			
Riboswitch	Biological Replicate	Negative	Arabinose	Theophylline	Arabinose & Theophylline
RboC	1	0.30	0.17	0.17	0.33
	2	0.10	0.17	0.07	0.10
	3	0.17	0.27	0.23	0.37
RboD	1	0.17	0.30	0.17	0.27
	2	0.33	0.20	0.30	0.43
	3	0.20	0.17	0.23	0.30
RboE	1	0.17	0.27	0.37	0.57
	2	0.10	0.33	0.40	0.20
	3	0.20	0.20	0.40	0.13

PHB Standard

	Area[µV.Min]		
PHB	Reading 1	Reading 2	Reading 3
0 µg	0.2	0.2	0.1
20 µg	3	3	2.9
40 µg	58	6.0	6.0
60 µg	9.5	8.8	9.1
80 µg	14.3	14.3	14.3
100 µg	22.7	22.6	22.7

Previously, detection of PHB production in *C. necator* has been demonstrated numerous times in WT cultures during optimization experiments. Issues in PHB detection only arose in ΔphaC *C. necator* transformed with plasmid constructs. PHB production in ΔphaC *C. necator* transformed with a plasmid construct was only detected once in the previously discussed preliminary result (*Figure 23* & *Table 4*), which had significant issues and was determined to be unreliable based on optimization experiments. A likely culprit for this failure is the cmyc tag fused to the N-terminus of phaC which may disrupt its function. The cmyc tag was intentionally included in all plasmid constructs for two reasons. The first reason was for western blotting ease as cmyc antibodies are established antibodies that had been purchased previously in our lab. The second, and more significant, reason was that the cmyc tag was also included in the plasmid constructs given to us by the laboratory of Dr. Golden. Based on literature review[21,68] there was significant concern that changing the sequence directly downstream of the riboswitches may cause them to be non-functional. This concern is validated when considering that changing the GOI (which is further downstream than the cmyc tag) did have a significant impact on riboswitch functionality.

5 Study Strengths and Limitations

There are areas of uncertainty regarding some of the results in this thesis. One area of uncertainty is that experimental procedures could have been further optimized, which may have had an impact on results. Optimization of growth conditions, for example, used pBADT-RboE-phaC to determine optimal L-arabinose and theophylline concentrations. RboE was used for this due to the successful results from FACS, and it was only later discovered that RboE was non-functional in phaC production. As riboswitch functionality

can be impacted by altering the GOI, all of the riboswitches should have been used for the optimization steps instead of just one. Furthermore, when *C. necator* cultures were inoculated for PHB production, the M9 media already contained L-arabinose and theophylline upon inoculation. This was an experimental error, as the cultures were forced to produce phaC before growth conditions were nitrogen depleted to encourage PHB production. Instead, the cultures should have grown for 24 hours before being exposed to L-arabinose and/or theophylline at the same time as the excess glucose was added. Although this may have impacted PHB production, it doesn't explain the complete absence of PHB, as some (albeit reduced) production should still have occurred if the enzyme was functioning properly. Still, it is important to note that optimization could have been improved.

Another area of uncertainty comes from the plasmid conformation. Restriction conformation was ambiguous for both pBADT-RboC-YFP and pBADT-RboD-YFP post *C. necator* transformation. Therefore, the lack of YFP expression could be attributed to cloning error, although, this is unlikely as plasmids were confirmed in NEB5α prior to transformation in *C. necator*. Furthermore, plasmid constructs were not sequenced due to a combination of time restraints and issues regarding the cryptic bands and *C. necator* isolation. Cryptic bands were initially thought to be contamination and may impact sequencing results. Sequencing should also be done post *C. necator* transformation to ensure the correct plasmid was transformed. Sequencing was planned for after these issues had been resolved. Unfortunately, resolving these issues took longer than anticipated, and due to time constraints exacerbated by COVID, it was deemed a higher priority to generate results for FACS, western blotting, and GC.

Despite these technical and conceptual challenges, a large aspect of this thesis work was to demonstrate that riboswitches are capable of functioning in the industrially relevant bacteria *C. necator*, something that to our knowledge has not been demonstrated previously. This has now been confirmed through both fluorescent reporter genes as well as western blotting. However, riboswitch variants had varying degrees of success based primarily on the downstream GOI. Riboswitches are often referred to as having plug-and-play functionality in literature.[14,15,21] Although this is true to some extent, they may not be as universal as we hoped for. In this work, changing the GOI downstream of the riboswitches greatly impacted riboswitch functionality. This demonstrates a potential pitfall that may impact further research, as well as highlights a significant gap in current research. Riboswitches have primarily been used in proof-of-concept experiments using reporter genes,[21] which may not be a reliable method for characterizing riboswitch functionality when considering their use for practical applications. Initial screening with reporter genes may be misleading, as it was for this thesis work. Therefore, as demonstrated in this work, investigating the range of riboswitch variants directly controlling the desired GOI(s) would be a far more effective approach.

Unfortunately, PHB production was only detected once during a preliminary experiment that had significant challenges as previously discussed. Despite numerous other attempts, this result was never able to be replicated. Standards were reliable and PHB was demonstrated to be produced by WT *C. necator* under numerous conditions. Furthermore, phaC production was demonstrated during western blotting, confirming the inducible system functioned properly. As previously discussed, a likely cause of this issue may be the cmyc-tag severely inhibiting the functionality of the phaC enzyme. However, removal

of the cmyc-tag may impact riboswitch functionality as demonstrated in this thesis and in literature.[21,68] It is therefore advisable to alter the sequences as little as possible. For example, altering the START codon so that translation occurs at the GOI rather than at the cmyc-tag would be less likely to impact riboswitch functionality compared to the entire removal of the cmyc-tag. Another solution that has incredible promise, but would require a significant amount of time and effort, would be the use of computer modelling, screening methods, and semi-random mutagenesis to create an ideal riboswitch for the production of phaC in *C. necator*. These methods have been used with significant success in the past for optimizing riboswitch functionality,[15,27,28] and could therefore be incredibly useful tools in the creation of a riboswitch optimized specifically for this industrial application.

6 Conclusion

As outlined in Hypothesis and Objectives, the overarching goal of this thesis was to demonstrate the potential of riboswitches as useful biological devices in industrial applications. This had three specific aims: (1) Regulation of gene expression in *C. necator* using theophylline riboswitches. (2) Expression of the industrially relevant enzyme phaC controlled by theophylline riboswitches in a ΔphaC *C. necator* strain. (3) Production of PHB in ΔphaC *C. necator* controlled by theophylline riboswitches. The first aim was accomplished during the FACS experiments which clearly showed RboE as functional for production of YFP. This was further enforced with the success of aim 2, when RboC and RboD demonstrated phaC production during western blotting. The third aim, however, was unable to be achieved, but this failure is most likely caused by non-functional myc-phaC rather than a failure of the riboswitch. Despite this failure, the overall goal to demonstrates the potential of a riboswitch in industrial applications was still achieved.

Although there is uncertainty regarding some of the results presented in this thesis, and although optimization could have been improved, this work was still able to demonstrate that synthetic riboswitches do have a large degree of potential as a biological tool (albeit less than hoped). Plug-and-play functionality was confirmed in a novel bacterial cell line and in the production of a novel gene relevant to industrial purposes. Although PHB production was unable to be confirmed, this is likely a fault of the fusion protein and not a fault of the riboswitches directly. It is clear that more optimization should be done before the full potential of the riboswitch can be utilized, and that current screening techniques involving reporter genes are not as reliable as literature may indicate. Still, this work demonstrates a large degree of potential for the practical application of synthetic riboswitches for industrial purposes.

7 Future Directions

This thesis provides justification to further explore the capabilities of the riboswitch for industrial applications. *C. necator* has now been demonstrated to be capable of controlling gene expression through riboswitches, but the riboswitches in this thesis could be improved upon. As stated previously, a combination of computer modeling, semi-random mutagenesis, and different screening processes could be used to design a synthetic riboswitch ideal for phaC expression in *C. necator*, as these methods have been used successfully in the past.[15,27,28] This could also expand upon the types of induction that could be implemented, such as designing riboswitches that operate through different ligands or thermosensing switches. Cost of production is currently a major limitation in bioplastic production,[69] using thermosensing switches would allow inducible expression without the purchase of chemical inducers. With enough time and resources, designing synthetic

riboswitches specifically for PHB production opens a wide range of possibilities and directions.

Although designing these complex riboswitches has a large degree of potential, it would also cost significant research and development, and there are other more immediate paths that could be taken that require less of an investment. Sequencing the plasmid constructs that were cloned would remove some uncertainty in the results of this thesis. Repeating some of the experiments with the previously discussed optimization steps (see Discussion) would also be valuable to help PHB production. An important step would be to demonstrate that the control of PHB production is capable through riboswitches, to directly show the power of the riboswitch for production of value-added goods. This thesis failed to demonstrate this, with the most likely cause for the failure is the cmyc-phaC fusion. A relatively simple experiment would be to alter the START codon of the cmyc-tag so that translation occurs at phaC. A single point mutation would likely have no impact (or a minimal impact) on the riboswitch structure while creating a functional phaC enzyme not fuzzed to a cmyc-tag. Preforming Selective 2′-hydroxyl acylation analyzed by primer extension (SHAPE) would provide significant insight into the structure-function of the riboswitches. Riboswitch function is clearly impacted by the GOI, and SHAPE is a technique that provides information on RNA folding and structure. This could clarify the mechanism that caused the loss-of-function in RboC-YFP, RboD-YFP, and RboE-phaC. The information obtained by SHAPE would also be incredibly valuable for computer modeling and other future directions.

8 References

1. Keshava, R., Mitra, R., Gope, M. L. & Gope, R. Synthetic Biology. in *Omics Technologies and Bio-Engineering* 63–93 (Elsevier, 2018). doi:10.1016/B978-0-12-804659-3.00004-X.
2. Andrianantoandro, E., Basu, S., Karig, D. K. & Weiss, R. Synthetic biology: new engineering rules for an emerging discipline. *Mol. Syst. Biol.* 2, 2006.0028 (2006).
3. Ausländer, S., Ausländer, D. & Fussenegger, M. Synthetic Biology-The Synthesis of Biology. *Angew Chem Int Ed Engl* 56, 6396–6419 (2017).
4. Freemont, P. S. Synthetic biology industry: data-driven design is creating new opportunities in biotechnology. *Emerg. Top. Life Sci.* 3, 651–657 (2019).
5. Endy, D. Synthetic biology: Can we make biology easy to engineer? *Industrial Biotechnology* 4, 340–351 (2008).
6. Grozinger, L. *et al.* Pathways to cellular supremacy in biocomputing. *Nat. Commun.* 10, 5250 (2019).
7. Friedman, D. C. & Ellington, A. D. Industrialization of Biology. *ACS Synth. Biol.* 4, 1053–1055 (2015).
8. Trinh, C. T. & Mendoza, B. Modular cell design for rapid, efficient strain engineering toward industrialization of biology. *Curr. Opin. Chem. Eng.* 14, 18–25 (2016).
9. Heinemann, M. & Panke, S. Synthetic biology--putting engineering into biology. *Bioinformatics* 22, 2790–2799 (2006).
10. Mukherji, S. & van Oudenaarden, A. Synthetic biology: understanding biological design from synthetic circuits. *Nat. Rev. Genet.* 10, 859–871 (2009).
11. Kitney, R. & Freemont, P. Synthetic biology - the state of play. *FEBS Lett.* 586, 2029–2036 (2012).
12. Stephanopoulos, G. Synthetic biology and metabolic engineering. *ACS Synth. Biol.* 1, 514–525 (2012).
13. Marchisio, M. A. & Stelling, J. Computational design tools for synthetic biology. *Curr. Opin. Biotechnol.* 20, 479–485 (2009).
14. Frasch, H.-J., Medema, M. H., Takano, E. & Breitling, R. Design-based re-engineering of biosynthetic gene clusters: plug-and-play in practice. *Curr. Opin. Biotechnol.* 24, 1144–1150 (2013).
15. Etzel, M. & Mörl, M. Synthetic Riboswitches: From Plug and Pray toward Plug and Play. *Biochemistry* 56, 1181–1198 (2017).
16. Mironov, A. S. *et al.* Sensing small molecules by nascent RNA: a mechanism to control transcription in bacteria. *Cell* 111, 747–756 (2002).
17. Nahvi, A. *et al.* Genetic control by a metabolite binding mRNA. *Chem. Biol.* 9, 1043 (2002).
18. Winkler, W., Nahvi, A. & Breaker, R. R. Thiamine derivatives bind messenger RNAs directly to regulate bacterial gene expression. *Nature* 419, 952–956 (2002).
19. Edwards, A. L. & Batey, R. T. Riboswitches: a common RNA regulatory element. *Nature Education* 3, (2010).
20. McCown, P. J., Corbino, K. A., Stav, S., Sherlock, M. E. & Breaker, R. R. Riboswitch diversity and distribution. *RNA* 23, 995–1011 (2017).

21. Nshogozabahizi, J. C., Aubrey, K. L., Ross, J. A. & Thakor, N. Applications and limitations of regulatory RNA elements in synthetic biology and biotechnology. *J. Appl. Microbiol.* 127, 968–984 (2019).
22. Chau, T. H. T., Mai, D. H. A., Pham, D. N., Le, H. T. Q. & Lee, E. Y. Developments of Riboswitches and Toehold Switches for Molecular Detection-Biosensing and Molecular Diagnostics. *Int. J. Mol. Sci.* 21, (2020).
23. Wachter, A. *et al.* Riboswitch control of gene expression in plants by splicing and alternative 3' end processing of mRNAs. *Plant Cell* 19, 3437–3450 (2007).
24. Breaker, R. R. Riboswitches and the RNA world. *Cold Spring Harb. Perspect. Biol.* 4, (2012).
25. Blouin, S., Chinnappan, R. & Lafontaine, D. A. Folding of the lysine riboswitch: importance of peripheral elements for transcriptional regulation. *Nucleic Acids Res.* 39, 3373–3387 (2011).
26. Groher, F. & Suess, B. Synthetic riboswitches - A tool comes of age. *Biochim. Biophys. Acta* 1839, 964–973 (2014).
27. Desai, S. K. & Gallivan, J. P. Genetic screens and selections for small molecules based on a synthetic riboswitch that activates protein translation. *J. Am. Chem. Soc.* 126, 13247–13254 (2004).
28. Topp, S. & Gallivan, J. P. Riboswitches in unexpected places--a synthetic riboswitch in a protein coding region. *RNA* 14, 2498–2503 (2008).
29. Hallberg, Z. F., Su, Y., Kitto, R. Z. & Hammond, M. C. Engineering and in vivo applications of riboswitches. *Annu. Rev. Biochem.* 86, 515–539 (2017).
30. Topp, S. *et al.* Synthetic riboswitches that induce gene expression in diverse bacterial species. *Appl. Environ. Microbiol.* 76, 7881–7884 (2010).
31. Ma, A. T., Schmidt, C. M. & Golden, J. W. Regulation of gene expression in diverse cyanobacterial species by using theophylline-responsive riboswitches. *Appl. Environ. Microbiol.* 80, 6704–6713 (2014).
32. Lynch, S. A. & Gallivan, J. P. A flow cytometry-based screen for synthetic riboswitches. *Nucleic Acids Res.* 37, 184–192 (2009).
33. Nelson, D. L. & Cox, M. M. Bioenergetics and Metabolsim. in *Principles of Biochemistry (Lehninger Principles of Biochemistry)* (W.H. Freeman, 2021).
34. Yadav, V. G., De Mey, M., Lim, C. G., Ajikumar, P. K. & Stephanopoulos, G. The future of metabolic engineering and synthetic biology: towards a systematic practice. *Metab. Eng.* 14, 233–241 (2012).
35. Lee, J. W. *et al.* Systems metabolic engineering of microorganisms for natural and non-natural chemicals. *Nat. Chem. Biol.* 8, 536–546 (2012).
36. Lee, J. W., Kim, T. Y., Jang, Y.-S., Choi, S. & Lee, S. Y. Systems metabolic engineering for chemicals and materials. *Trends Biotechnol.* 29, 370–378 (2011).
37. Chae, T. U., Choi, S. Y., Kim, J. W., Ko, Y.-S. & Lee, S. Y. Recent advances in systems metabolic engineering tools and strategies. *Curr. Opin. Biotechnol.* 47, 67–82 (2017).
38. Choi, S. Y. *et al.* One-step fermentative production of poly(lactate-*co*-glycolate) from carbohydrates in *Escherichia coli*. *Nat. Biotechnol.* 34, 435–440 (2016).
39. Galanie, S., Thodey, K., Trenchard, I. J., Filsinger Interrante, M. & Smolke, C. D. Complete biosynthesis of opioids in yeast. *Science* 349, 1095–1100 (2015).
40. Atsumi, S. *et al.* Metabolic engineering of Escherichia coli for 1-butanol production.

Metab. Eng. 10, 305–311 (2008).
41. Hanai, T., Atsumi, S. & Liao, J. C. Engineered synthetic pathway for isopropanol production in Escherichia coli. *Appl. Environ. Microbiol.* 73, 7814–7818 (2007).
42. Nies, D. H. Microbial heavy-metal resistance. *Appl. Microbiol. Biotechnol.* 51, 730–750 (1999).
43. Tibazarwa, C., Wuertz, S., Mergeay, M., Wyns, L. & van Der Lelie, D. Regulation of the cnr cobalt and nickel resistance determinant of Ralstonia eutropha (Alcaligenes eutrophus) CH34. *J. Bacteriol.* 182, 1399–1409 (2000).
44. Ammann, E. C. B. & Reed, L. L. Metabolism of nitrogen compounds by hydrogenomonas eutropha. *Biochimica et Biophysica Acta (BBA) - General Subjects* 141, 135–143 (1967).
45. Chen, G.-Q. A microbial polyhydroxyalkanoates (PHA) based bio- and materials industry. *Chem. Soc. Rev.* 38, 2434–2446 (2009).
46. Karamanlioglu, M., Preziosi, R. & Robson, G. D. Abiotic and biotic environmental degradation of the bioplastic polymer poly(lactic acid): A review. *Polym. Degrad. Stab.* 137, 122–130 (2017).
47. Kalia, V. C., Chauhan, A., Bhattacharyya, G. & Rashmi. Genomic databases yield novel bioplastic producers. *Nat. Biotechnol.* 21, 845–846 (2003).
48. Mothes, G., Schnorpfeil, C. & Ackermann, J. U. Production of PHB from Crude Glycerol. *Eng. Life Sci.* 7, 475–479 (2007).
49. Peoples, O. P. & Sinskey, A. J. Poly-β-hydroxybutyrate (PHB) biosynthesis in Alcaligenes eutrophus H16. *Journal of Biological Chemistry* 264, 15298–15303 (1989).
50. Kumari, A. Glycolysis. in *Sweet Biochemistry* 1–5 (Elsevier, 2018). doi:10.1016/B978-0-12-814453-4.00001-7.
51. Humphreys, C. M. & Minton, N. P. Advances in metabolic engineering in the microbial production of fuels and chemicals from C1 gas. *Curr. Opin. Biotechnol.* 50, 174–181 (2018).
52. Shin, G. *et al.* Biosynthesis of Polyhydroxybutyrate with Cellulose Nanocrystals Using Cupriavidus necator. *Polymers (Basel)* 13, 2604 (2021).
53. Špoljarić, I. V. *et al.* Mathematical modeling of poly[(R)-3-hydroxyalkanoate] synthesis by Cupriavidus necator DSM 545 on substrates stemming from biodiesel production. *Bioresour. Technol.* 133, 482–494 (2013).
54. Khosravi-Darani, K., Vasheghani-Faraahani, E. & Shojaosadati, S. A. Application of the Taguchi Design for Production of Poly(β-hydroxybutyrate) by Ralstonia eutropha. *IJCCE* 23, (2004).
55. Batcha, A. F. M., Prasad, D. M. R., Khan, M. R. & Abdullah, H. Biosynthesis of poly(3-hydroxybutyrate) (PHB) by Cupriavidus necator H16 from jatropha oil as carbon source. *Bioprocess Biosyst. Eng.* 37, 943–951 (2014).
56. Rodríguez-Contreras, A. *et al.* Influence of glycerol on poly(3-hydroxybutyrate) production by *Cupriavidus necator* and *Burkholderia sacchari*. *Biochem. Eng. J.* 94, 50–57 (2015).
57. Verlinden, R. A. J., Hill, D. J., Kenward, M. A., Williams, C. D. & Radecka, I. Bacterial synthesis of biodegradable polyhydroxyalkanoates. *J. Appl. Microbiol.* 102, 1437–1449 (2007).
58. Volova, T. G., Kalacheva, G. S. & Altukhova, O. V. Autotrophic synthesis of

polyhydroxyalkanoates by the bacteria Ralstonia eutropha in the presence of carbon monoxide. *Appl. Microbiol. Biotechnol.* 58, 675–678 (2002).
59. Aramvash, A., Moazzeni Zavareh, F. & Gholami Banadkuki, N. Comparison of different solvents for extraction of polyhydroxybutyrate from Cupriavidus necator. *Eng. Life Sci.* 18, 20–28 (2018).
60. Pradhan, S., Dikshit, P. K. & Moholkar, V. S. Production, ultrasonic extraction, and characterization of poly (3-hydroxybutyrate) (PHB) using *Bacillus megaterium* and *Cupriavidus necator*. *Polym. Adv. Technol.* 29, 2392–2400 (2018).
61. Alejandra, R.-C., Margarita, C.-M. & María Soledad, M.-C. Enzymatic degradation of poly(3-hydroxybutyrate) by a commercial lipase. *Polym. Degrad. Stab.* 97, 2473–2476 (2012).
62. Juengert, J., Bresan, S. & Jendrossek, D. Determination of Polyhydroxybutyrate (PHB) Content in Ralstonia eutropha Using Gas Chromatography and Nile Red Staining. *Bio Protoc* 8, (2018).
63. Lo, C.-W., Wu, H.-S. & Wei, Y.-H. Optimizing acidic methanolysis of poly(3-hydroxyalkanoates) in gas chromatography analysis. *Asia-Pacific Jrnl of Chem. Eng* 4, 487–494 (2009).
64. Braunegg, G., Sonnleitner, B. & Lafferty, R. M. A rapid gas chromatographic method for the determination of poly-*β*-hydroxybutyric acid in microbial biomass. *European J. Appl. Microbiol. Biotechnol.* 6, 29–37 (1978).
65. Reusch, R. N. The role of short-chain conjugated poly-(R)-3-hydroxybutyrate (cPHB) in protein folding. *Int. J. Mol. Sci.* 14, 10727–10748 (2013).
66. Tian, J. *et al.* Analysis of transient polyhydroxybutyrate production in Wautersia eutropha H16 by quantitative Western analysis and transmission electron microscopy. *J. Bacteriol.* 187, 3825–3832 (2005).
67. Sayers, J. R., Evans, D. & Thomson, J. B. Identification and eradication of a denatured DNA isolated during alkaline lysis-based plasmid purification procedures. *Anal. Biochem.* 241, 186–189 (1996).
68. Folliard, T. *et al.* Ribo-attenuators: novel elements for reliable and modular riboswitch engineering. *Sci. Rep.* 7, 4599 (2017).
69. Chee, J. Y., Yoga, S. S., Lau, N. S., Ling, S. C. & Sudesh, K. (PDF) Bacterially produced polyhydroxyalkanoate (PHA): Converting renewable resources into bioplastic. *Current research, technology and education topics in Applied Microbiology and Microbial Biotechnology, 2, 1395-1404.* (2010).

Appendix 1 Plasmid maps of pBADT-RboS-YFP & pBADT-RboS-phaC.